

AD-A065 897

AIR FORCE FLIGHT DYNAMICS LAB WRIGHT-PATTERSON AFB OHIO  
A LASER-INDUCED LIGHTNING CONCEPT EXPERIMENT. (U)

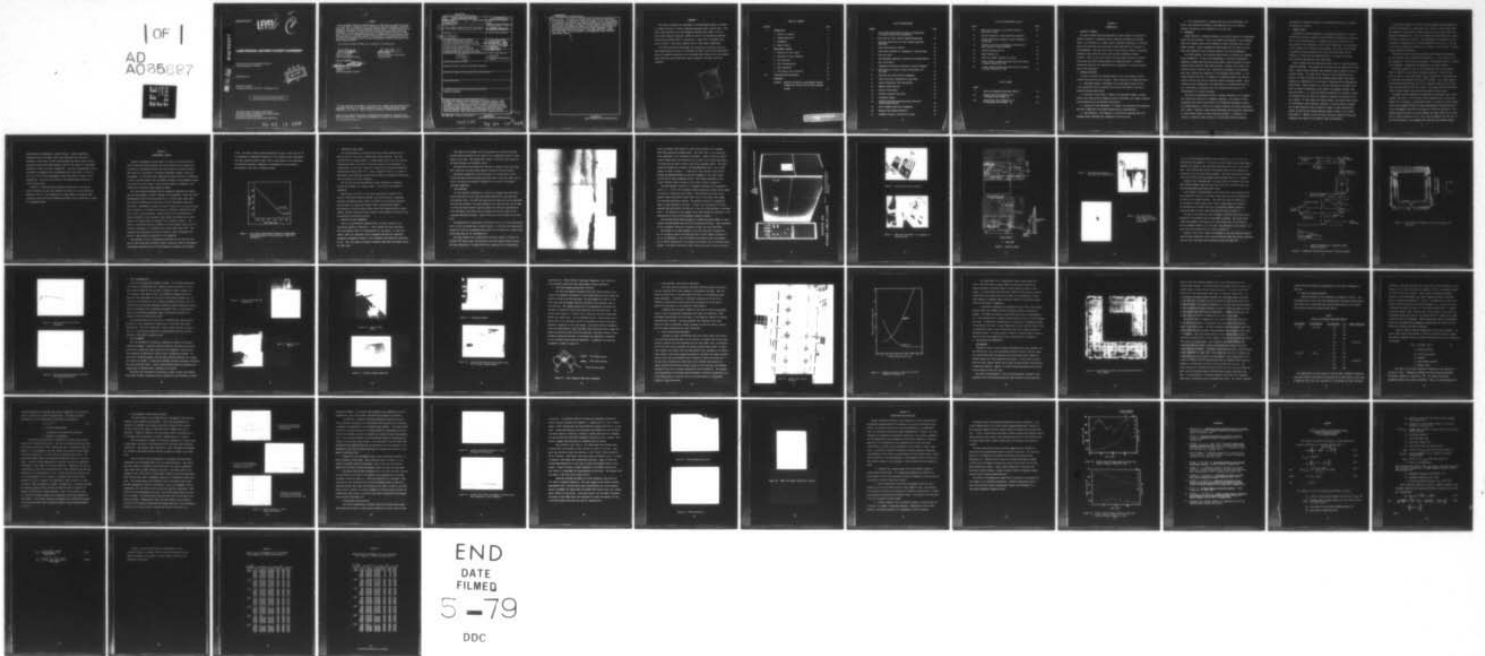
F/G 4/1

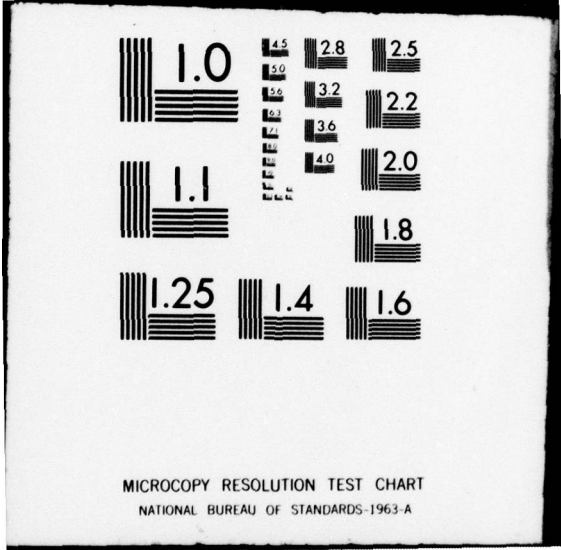
UNCLASSIFIED

DEC 78 J R LIPPERT  
AFFDL-TR-78-191

NL

1 OF 1  
AD A065897  
DTIC





MICROCOPY RESOLUTION TEST CHART  
NATIONAL BUREAU OF STANDARDS-1963-A

AFFDL-TR-78-191

**LEVEL**

②

AD A0 65897

**LASER-INDUCED LIGHTNING CONCEPT EXPERIMENT**

*SURVIVABILITY/VULNERABILITY BRANCH  
VEHICLE EQUIPMENT DIVISION*

DECEMBER 1978

TECHNICAL REPORT  
Final Report for Period 1 May 1977 - 30 September 1977

DDC  
RECEIVED  
MAR 19 1979  
C

DDC FILE COPY

Approved for public release; distribution unlimited.

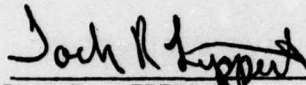
AIR FORCE FLIGHT DYNAMICS LABORATORY  
AIR FORCE WRIGHT AERONAUTICAL LABORATORIES  
AIR FORCE SYSTEMS COMMAND  
WRIGHT-PATTERSON AIR FORCE BASE, OHIO 45433

79 03 13 047

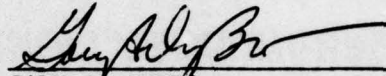
NOTICE

When Government drawings, specifications, or other data are used for any purpose other than in connection with a definitely related Government procurement operation, the United States Government thereby incurs no responsibility nor any obligation whatsoever; and the fact that the government may have formulated, furnished, or in any way supplied the said drawings, specifications, or other data, is not to be regarded by implication or otherwise as in any manner licensing the holder or any other person or corporation, or conveying any rights or permission to manufacture, use, or sell any patented invention that may in any way be related thereto.

This report has been reviewed and is approved for publication.



JACK R. LIPPERT  
Aerospace Engineer  
Vehicle Equipment Division



GARY A. DUBRO  
Chief, Atmospheric Electricity  
Hazards Group

FOR THE COMMANDER



AMBROSE B. NUTT  
Director  
Vehicle Equipment Division

"If your address has changed, if you wish to be removed from our mailing list, or if the addressee is no longer employed by your organization please notify AFFDL/FES, W-P AFB, OH 45433 to help us maintain a current mailing list".

Copies of this report should not be returned unless return is required by security considerations, contractual obligations, or notice on a specific document.

UNCLASSIFIED

SECURITY CLASSIFICATION OF THIS PAGE (When Data Entered)

REPORT DOCUMENTATION PAGE		READ INSTRUCTIONS BEFORE COMPLETING FORM
1. REPORT NUMBER AFFDL-TR-78-191	2. GOVT ACCESSION NO.	3. RECIPIENT'S CATALOG NUMBER 9
4. TITLE (and Subtitle) A Laser-Induced Lightning Concept Experiment	5. TYPE OF REPORT & PERIOD COVERED Final rept. 1 May - 30 Sep 77	
7. AUTHOR(s) Jack R. Lippert	8. CONTRACT OR GRANT NUMBER(s)	
9. PERFORMING ORGANIZATION NAME AND ADDRESS Air Force Flight Dynamics Laboratory AF Wright Aeronautical Laboratories, AFSC Wright-Patterson Air Force Base, Ohio 45433	10. PROGRAM ELEMENT, PROJECT, TASK AREA & WORK UNIT NUMBERS Program Element 62201F Project 2402 Task 02 Work Unit 2402022	11. REPORT DATE December 1978
11. CONTROLLING OFFICE NAME AND ADDRESS Air Force Flight Dynamics Laboratory AF Wright Aeronautical Laboratories, AFSC Wright-Patterson Air Force Base, Ohio 45433	12. NUMBER OF PAGES 12 58p.	
14. MONITORING AGENCY NAME & ADDRESS (if different from Controlling Office)	15. SECURITY CLASS. (of this report) UNCLASSIFIED	
16. DISTRIBUTION STATEMENT (of this Report) Approved for public release; distribution unlimited		
17. DISTRIBUTION STATEMENT (of the abstract entered in Block 20, if different from Report)		
18. SUPPLEMENTARY NOTES		
19. KEY WORDS (Continue on reverse side if necessary and identify by block number) Lightning Triggering		
20. ABSTRACT (Continue on reverse side if necessary and identify by block number) A program was conducted to gain experience and document progress towards development of a concept for a Laser-Induced Lightning Experiment (LILE). The purpose of the program was to develop a method for triggering natural lightning discharges using pulsed lasers and verify theoretical predictions. The technique shows great promise in shortening the acquisition period for obtaining necessary lightning parameter data needed for more realistic Lightning Simulation Tests (LST) and more definitive Lightning Transient		

DD FORM 1473 EDITION OF 1 NOV 65 IS OBSOLETE

UNCLASSIFIED

SECURITY CLASSIFICATION OF THIS PAGE (When Data Entered)

012 070

79 03 13 047 LB

**UNCLASSIFIED**

SECURITY CLASSIFICATION OF THIS PAGE(When Data Entered)

Analyses (LTA). To achieve the intended objective within the restrictions of availability, an experimental method was designed, a test locale selected, test parameters were defined, test apparatus designed and test instrumentation selected and/or developed. Although the required climatic conditions did not develop during the experimental period, all other phases of the program were successfully accomplished and will facilitate future experiments. Small scale experiments were also performed to investigate spark gap triggering using laser beams, laser beam effects on electromagnetic fields, and laser power/energy scaling.

**UNCLASSIFIED**

SECURITY CLASSIFICATION OF THIS PAGE(When Data Entered)

**FOREWORD**

This report documents the development of an experimental method to attempt to trigger and direct a natural lightning discharge using a pulsed laser. This effort was performed by the Electromagnetic Hazards Group (FES) of the Air Force Flight Dynamics Laboratory (AFFDL) as part of the Thunderstorm Research International Program (TRIP 77) during July - August 1977, at Kennedy Space Center, Florida. The project engineer was Mr. Jack Lippert (AFFDL/FES)

The author gratefully acknowledges the cooperation of personnel from the NASA Langley Research Center for providing the laser, the Air Force Orientation Group for logistics assistance, and the Kennedy Space Center for on-site support. These concerted efforts made this project possible in the short lead time available.

ACCESSION for	White Section	<input checked="" type="checkbox"/>
NTIS	Buff Section	<input type="checkbox"/>
100		<input type="checkbox"/>
UNCLASSIFIED		
CONFIDENTIAL		
BY	DISTRIBUTION PRIORITY CODES	
		SPECIAL
A		

## TABLE OF CONTENTS

SECTION		PAGE
I	INTRODUCTION	1
	1. Purpose of Program	1
	2. Program Objectives	1
	3. Background	2
	4. General Theory	3
II	EXPERIMENTAL CONCEPT	6
	1. Selection of Test Locale	8
	2. Selection of Test Parameters	8
	3. Test Apparatus	9
	4. Test Instrumentation	20
	5. Test Procedures	20
	6. Test Results and Correlation	28
III	CONCLUSIONS AND DISCUSSIONS	41
	REFERENCES	44
	APPENDIX ANALYSIS OF SPECIFIC LASER-INDUCED IONIZED PATHWAYS AND TYPICAL DATA FOR ONE KILOMETER PATHWAY	45

## LIST OF ILLUSTRATIONS

FIGURE		PAGE
1	Flux Versus Pulse-Length Criterion for Maintenance of Rarefied Channel by CO <sub>2</sub> Radiation	7
2	Power Used for Laser Induced Lightning Experiment	10
3	CO <sub>2</sub> Laser System Used for Laser Induced Lightning Experiment	12
4	Laser System Control Console	13
5	HeNe Laser Attachment for Alignment of Infrared Laser	13
6	Facility Layout	14
7	Beam Expanding Cassegrain Telescope and Pointing Mirror	15
8	Flat Field Mirror	15
9	Dimensions and Relative Positions of Optical Elements	17
10	Beam Pattern of System, Science and Software (S <sup>3</sup> ) CO <sub>2</sub> Laser	18
11	Beam Path from Semi-Trailer Arrangement	19
12	Tower Electrodes Illuminated by Light Beam	19
13	Current Transformer (CT) Installation	21
14	Magnetic Field Detector	21
15	Electric Field Dipole	22
16	Potential Gradient Field Mill	22
17	Stormscope Display	23
18	Transient Recorder and Oscilloscope Setup with Typical Signal Display	23
19	Laser Triggered Spark Gap Arrangement	24
20	Megavolt Marx Impulse Generator	26
21	Breakdown Criteria, Clean Air at 10.6μm	27

LIST OF ILLUSTRATIONS (Cont'd)

FIGURE		PAGE
22	Beam Pattern of Army's Cold Cathode Electron Beam Laser (CCEBL)	29
23	Typical Responses at Three Beam Focus Distances	35
24	Current Transformer Response to Marx Discharge of 20,000 Amps	37
25	Electric (Top Trace) and Magnetic (Bottom Trace) Field Response to Marx Discharge	37
26	Florida Demonstration Arc	39
27	CCEBL Produced Arc	39
28	CCEBL "Arc Beads" Produced at 10 Hertz	40
29	24-Hour Signal Strength and Pulse Count Plot During a Tornado, January 28, 1973	43
30	24-Hour Signal Strength and Pulse Count Plot During a Tornado, February 6, 1973	43

LIST OF TABLES

TABLE		
1	Spark Gap Triggering Experiment Results	31
A-1	Typical Laser Rod Parameters for a 1 Kilometer Focal Length, $Z_F$	49
A-2	Typical Laser Rod Parameters for a 0-5 Kilometer Focal Length, $Z_F$	50

## SECTION I

### INTRODUCTION

#### 1. PURPOSE OF PROGRAM

The Laser Induced Lightning Experimental (LILE) program was intended to develop a method for triggering natural lightning discharges using pulsed lasers. The capability to trigger natural lightning discharges at a selected locale will facilitate the collection of much needed data on the nature of this phenomenon. The data can be used to attain greater realism in lightning simulation tests (LST) and, hence, more accurate lightning transient analyses. This, in turn, will result in better design criteria for protecting aircraft and other systems against the lightning hazard. Although a theoretical basis for this approach exists, experiments to verify the theory had not been conducted.

#### 2. PROGRAM OBJECTIVES

In order to achieve the intended purpose of the LILE program, several related objectives had to be attained. These objectives are summarized below:

- a. Experiment Design - Development of an experimental method was the first requirement since no previous work had been performed in the area of inducing lightning with lasers.
- b. Selection of Test Locale - Based on the experiment design, an appropriate test locale with the required terrain, environment, and support personnel and facilities had to be specified and selected.
- c. Selection of Test Parameters - To support the experiment, test parameters and their ranges had to be defined analytically or experimentally.
- d. Test Apparatus - Test apparatus to perform the experiment had to be designed and/or specified and transported to the test site.

e. Test Instrumentation- To measure and record test measurements and monitor test apparatus performance, instrumentation had to be selected, acquired, checked out, and transported to the test site.

### 3. BACKGROUND

A major obstacle in lightning studies is the erratic nature of the phenomenon itself and its occurrence. Due to the inherent uncertainties of the discharge times and locations, years may be required to obtain sufficient data on even distant strikes. Several schemes have been devised over the years to obtain close hand examination and accelerate studies of the natural phenomenon.

In initial studies, tall structures were erected to increase the lightning strike probability. In more active approaches to artificial triggering of lightning, attempts were made using water plumes, tethered ballons and rocker launched wires, each with some limited success. However, each concept that involves an ohmic conductor over a substantial percentage of the discharge path risks altering some parameters of the phenomena being studied. In the rocket-launched wire case, for example, the lightning current will promptly vaporize the wire and form an ionization channel of metallic plasma. Due to conductivity and recombination rate differences of the plasma from those of air, there exists a probability that the resulting strike would not be representative of a natural discharge.

The ability of high-powered lasers to produce ionization in air suggests that they may be effective in triggering lightning. The process of laser triggering would theoretically result in the lightning following an ionized air pathway similar in nature to the channel formed by the natural lightning's pilot leader. Therefore, laser-induced discharges should provide an opportunity to study strikes similar to those occurring naturally. In addition, the ability to choose the time and place of the discharge without injecting

substances not ordinarily present will substantially increase the quantity and quality of the data.

#### 4. GENERAL THEORY

Although the precise mechanisms of a lightning discharge are currently undefined one can gain insight into the phenomena by comparing the clouds and earth to the parallel plates of a capacitor with an air dielectric (for the purpose of this experiment, cloud-to-cloud lightning is not considered). In this analogy as the "plates" become charged, the electric field between the ground and cloud increases until, when sufficiently high, the air "dielectric" breaks down and lightning occurs. In reality, of course, this process is substantially more complicated.

Several schemes have been postulated using a laser to cause the desired lightning discharge. The schemes can be divided into two applications of the laser: either produce ionization (an increased electron density) or form a rarefied channel. The laser can be focused to cause ionization from the ground to as high an altitude as the available power permits. This would simulate the conductivity of a tall tower or lightning rod by elevating the ground plane. Another method is to form the ionization at the base of the cloud in hopes of stimulating a pilot leader to propagate naturally from that point (Ref 1). A still more ambitious approach is to produce a column of ionization from the cloud to the ground to simulate the function of the pilot leader. If there exists any charge buildup, this method should result in a discharge as would shorting a capacitor (to use the earlier analogy). All of these methods are fast acting with regard to charge distribution, thereby introducing the assumed important dynamic changes to the present field (Ref 2). However, as will be shown, the power required to form this ionization over paths in the kilometer range is substantial.

A more subtle approach is to form a rarefied channel and thus weaken the "dielectric insulation" in a particular spot. Then as a pilot leader forms and propagates, it will tend to follow the easiest path to ground and break through this weakened spot. Since the formation and persistence time is short, the dynamic condition is retained. The disadvantage of this method is that it depends on lightning about to strike somewhere in the vicinity. The size of the vicinity affected is unknown, but is likely to be a function of channel strength (density) and height.

The details of laser produced ionization over kilometer-long pathways are quite complex and are published in Reference 3. In this section, only the highlights of this process are presented. Representative data is included in the Appendix to demonstrate the magnitude of the power required.

The data in Tables A-1 and A-2 were calculated based on the accepted value of  $3\text{GW}/\text{cm}^2$  for the clean air breakdown threshold. From the first entry in Table A-1, the power density ( $S_{\text{max}}$ ) required for a continuous path of ionization one kilometer long ( $Z_F$ ) is  $2.79\text{GW}/\text{cm}^2$ . For a laser pulse of one microsecond duration ( $t_E$ ) and a 8.21 cm aperture radius ( $W_L$ ) the total laser energy required is  $591 \times 10^3$  joules. This value results from multiplication of power density, pulse duration and aperture area values.

Although this power magnitude is obtainable by adding many laser outputs together, the result is of the same order of magnitude as an actual pilot leader and is, therefore, an undesirable option. It should be noted, however, that an air breakdown threshold has been experimentally observed with power in the 500 megawatt range and is attributed to "dirty air particles." By a similar process as used in the above example, the laser energy for the first four  $W_L$  values in Table A-2 at  $Z_B = 374\text{ m}$  can be computed to be 197, 94, 97 and 118 respectively. This suggests that aperture size dependent energy

minima exist for breakdown at a given distance. Another significant observation that can be made, which also demonstrates how the data in Reference 3 can be used, is that focusing range ( $Z_F$ ) has an effect on both the optics size and the power required, that in turn results in total power reduction of almost one order of magnitude. This can be demonstrated, as for an example, by comparing the corresponding values from Tables A-1 and A-2 at a  $Z_B$  of 375 m for the approximately equal size optics in lines 1 and 2, respectively. For these two conditions, the computed powers differ by a factor greater than 5.

Analysis of lightning fields gradients indicate that it is not the electron density, but the space gradient over which it acts that should be maximized. (Ref 4). This suggests that a long column of relatively weak ionization (levels far below breakdown threshold), may be sufficient to result in a discharge stroke.

## SECTION II

### EXPERIMENTAL CONCEPT

Because an experiment of this nature, at least on a full-scale basis, had not previously been performed, the first objective of the program was to develop an experimental concept that would result in a practical experiment within the constraints of available technology, hardware, locale and environment. It was decided that combining the subtle approach of attempting to form a rarefied channel with the gradual focusing to near breakdown intensities would be the best chance to cause a pilot leader to propagate in the chosen area at which the laser energy was aimed.

The subtle approach presented does not depend on ionization but rather uses the laser energy to rarefy a channel in the atmosphere. Since the "fast" recombination rates of free electrons are not a factor, laser pulse times are limited by diffusion and wind shear of the air molecules outside the laser beam. Experiments by Koopman and Saum<sup>5</sup> indicate that a rarefied channel must be lowered to .67 ambient air density to establish a preferential pathway to guide a spark discharge. Using this value, the approximate flux density required to form a kilometer-long channel was plotted versus pulse length for a channel radius by Schubert<sup>3</sup> and is shown in Figure 1. The effects of wind shear were not included as it would require longer than  $10^{-3}$  seconds to dissipate a 1 cm channel with a 20 mph (890 cm/sec) wind. The necessary flux intensities are further reduced at laser wavelengths that exhibit a high molecular attenuation in the atmosphere.

This approach, in turn, influenced the selection of the test site and time of year during which favorable climatic conditions could be anticipated. The approach permitted the use of laser energies attainable with portable

units. The energy levels required influenced the type of laser used as did the atmospheric transmission properties at the available laser wavelengths. The laser selection played a major role in other aspects of the experiment involving test apparatus components, instrumentation, and procedures, particularly in the area of personnel safety.

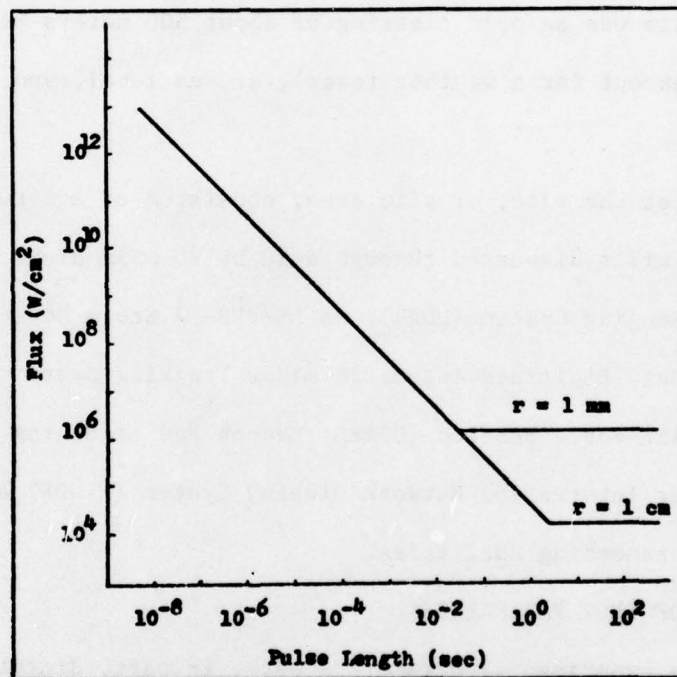


Figure 1. Flux Versus Pulse-Length Criterion for Maintenance of Rarefied Channel by CO<sub>2</sub> Radiation (Taken from Reference 3).

## 1. SELECTION OF TEST LOCALE

The LILE experiment was conducted at the Fire Rescue Training Area on Merritt Island at the John F. Kennedy Space Center, Florida. This site was selected for several reasons. Included among these is the fact that the thunderstorm season in the area is the most severe in the continental U.S. Consequently, the site was selected for conducting the Thunderstorm Research International Program (TRIP 77)<sup>6</sup>. Also, in support of TRIP 77, a number of experiments being conducted involved using research instrumentation whose data could be useful to the LILE experiment.

The test site was an open clearing of about 500 meters in diameter, totally flat (except for a weather tower), at sea level, and devoid of underbrush.

Facilities at the site, or site area, consisted of a network of 25 electric field mills dispersed through a 10 by 20 mile area, a Lightning Detection and Ranging System (LDAR), an AN/FPS-77 Storm Detection Meteorological Radar Set, Digitized Automatic Radar Tracking System (DARTS), Cape Canaveral Air Force Station (CCAFS) Launch Pad Lightning Warning System (LPLWS), Weather Information Network Display System (WINDS) and assorted data processing and recording facilities.

## 2. SELECTION OF TEST PARAMETERS

Some of the experimental parameters were, in part, dictated by the theoretical analysis of Reference 3. This included the laser wavelength (10.6 micrometers) which is a characteristic of CO<sub>2</sub> lasers. At this wavelength, there is a relatively low air breakdown threshold and reasonable atmospheric propagation because of the transmissive and absorptive properties of air. Also, CO<sub>2</sub> lasers are usually relatively high power and energy devices for their size.

The range of one kilometer for the experiment was partially dictated by the optical properties of the laser and the predominant ground to cloud height in the area. The maximum focal length of 500 meters was limited by the beam divergence and available optics.

The beam width and focusing were selected to maximize power and energy and to maintain the power energy density through the desired distance.

Horizontal propagation of the laser beam to a turning mirror 100 ft. distant and then directed through electrodes atop a fifty foot tower, was to protect the laser from possible "flashback" in the event of successful lightning triggering.

### 3. TEST APPARATUS

The test apparatus consisted of a fifty foot aluminum tower with three pointed electrodes on top, which was erected and guided by non-conductive polypropylene cords. The tower was sunk into the sandy soil and an additional grounding rod attached. The ohmic reading of the tower was less than 15 ohms to ground and would provide a positive hookup for analysis instrumentation while providing a more direct path to ground than the laser beam for any triggered lightning discharge. Figure 2 shows the tower erected at the test site.

The apparatus was transported to the Florida site in a 30 foot semi-trailer and a 25 foot van loaded atop a flatbed trailer. At the site, the semi-trailer housed the laser and propagating optics while the van served as a control room and Faraday cage for the instrumentation.

The laser employed was a commercially available Systems, a Science and Software (S<sup>3</sup>) model number 400 provided by the NASA Langley Research Center. The size limitation of the semi-trailer was compensated for by employing a

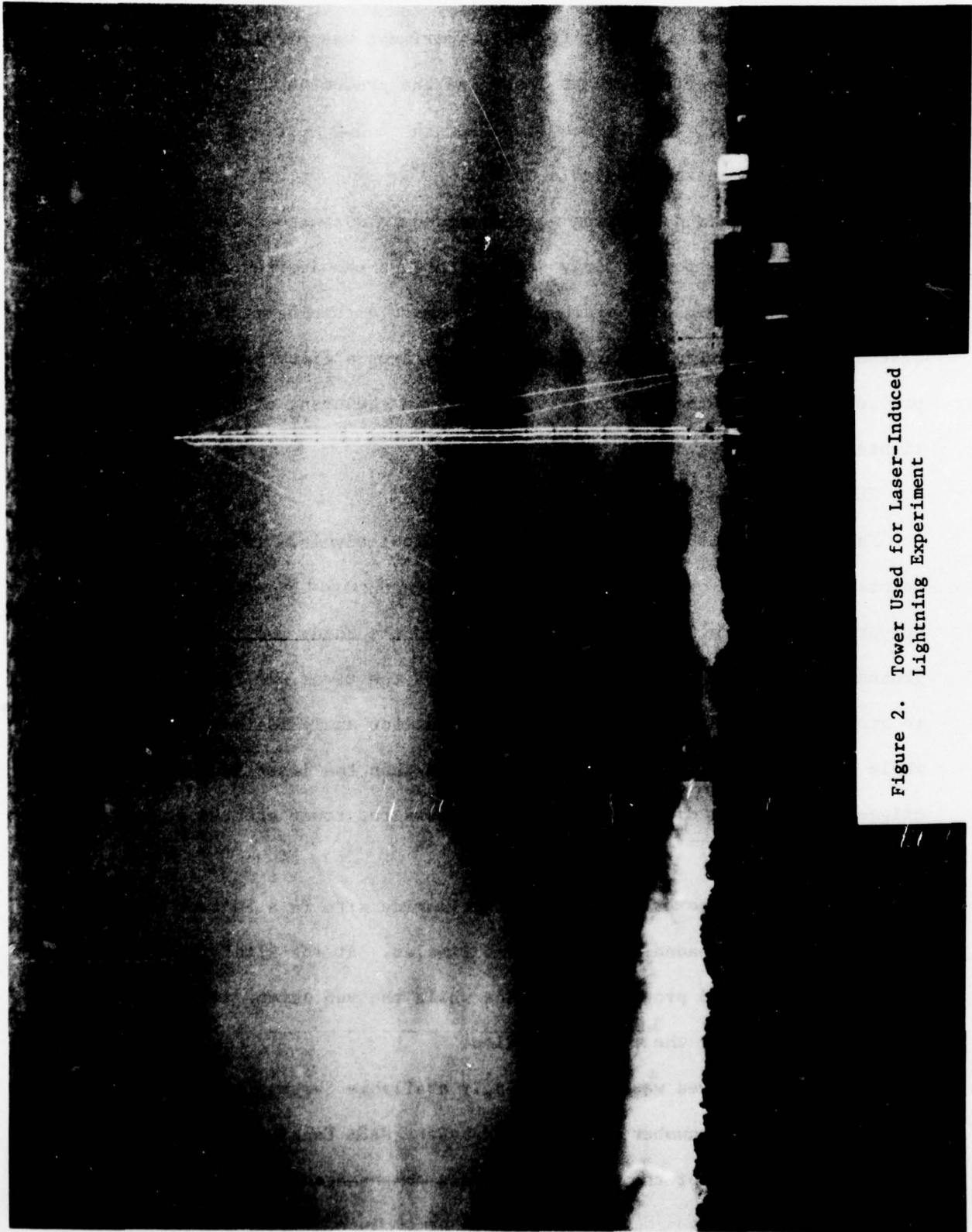


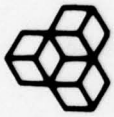
Figure 2. Tower Used for Laser-Induced  
Lightning Experiment

pulse transformer power supply for laser firing instead of the standard bulky Marx generator discharge supply. The laser (Fig. 3) is a pulsed CO<sub>2</sub> laser operating at 10.6 micrometers (infrared). Figure 4 shows the laser's control console which was installed in the control van for real-time control over detectors and laser firing as well as for personnel safety. The laser system was aligned by attaching a five milliwatt HeNe laser to the cavity bracket as shown in Figure 5. A 1mm hole in the resonator cavity mirror passing the HeNe beam allowed for positive alignment of the laser cavity mirrors and the beam propagation optics. The relative positions of the various hardware items are shown in the facility layout in Figure 6.

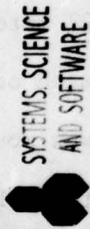
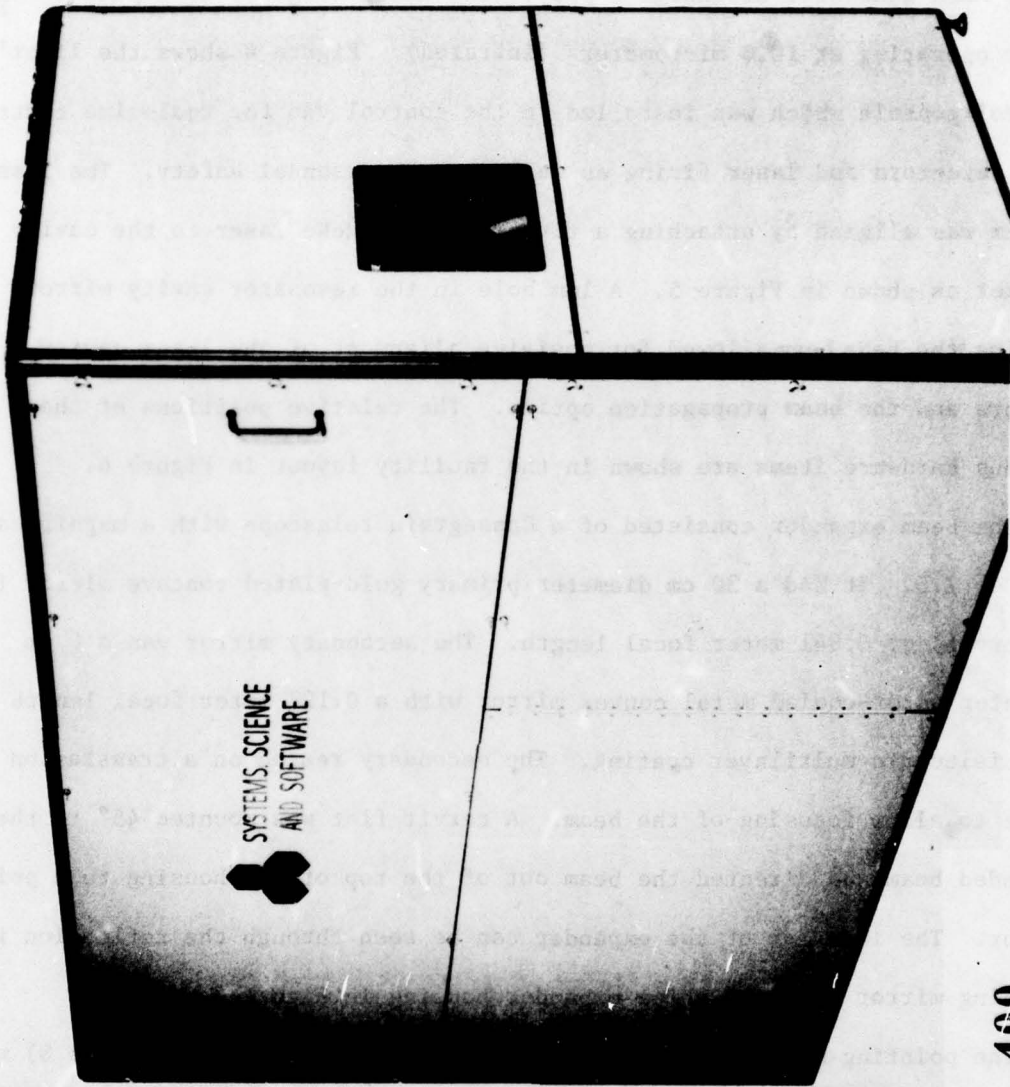
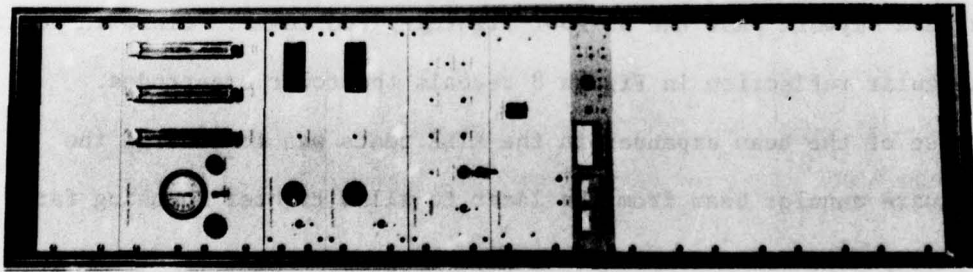
The beam expander consisted of a Cassegrain telescope with a magnification of 7.5. It had a 30 cm diameter primary gold-plated concave mirror (made of Cervit) of 0.841 meter focal length. The secondary mirror was a 6 cm diameter water-cooled metal convex mirror with a 0.127 meter focal length and dielectric multilayer coating. The secondary rested on a translation stage to allow focusing of the beam. A cervit flat was mounted 45° to the expanded beam and directed the beam out of the top of the housing to a pointing mirror. The interior of the expander can be seen through the reflection in the pointing mirror atop the white expander housing in Figure 7.

The pointing mirror aimed the beam at a field flat mirror (Figure 8) which relayed the beam skyward past the 50 foot lightning rod tower. Close inspection of the rectangular reflection in Figure 8 reveals the tower electrodes.

The purpose of the beam expander in the LILE tests was to enlarge the 10 x 10 cm square annular beam from the laser to allow tighter focusing far out in the atmosphere. Since the beam was too large to enter the expander in its normal configuration, the expander was reversed and the secondary mirror removed. Two double convex NaCl (salt) lenses were used to reduce the beam to



SYSTEMS, SCIENCE AND SOFTWARE



SYSTEMS, SCIENCE  
AND SOFTWARE

# SYSTEM 400 PULSED e-BEAM LASER

Figure 3. CO<sub>2</sub> Laser System Used for  
Laser-Induced Lightning  
Experiment

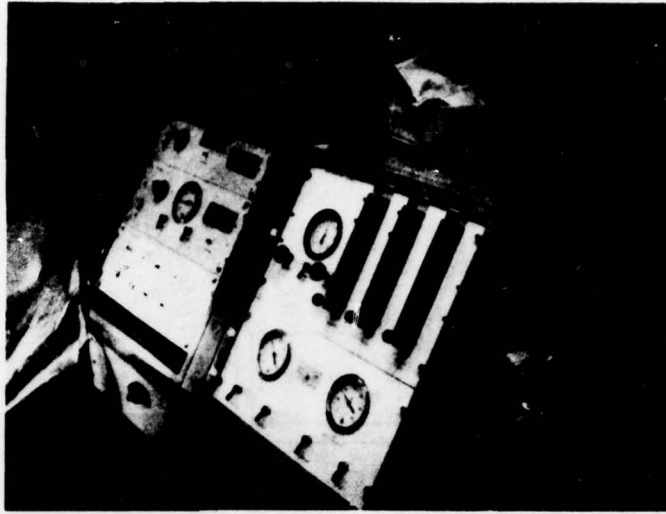


Figure 4. Laser System Control Console

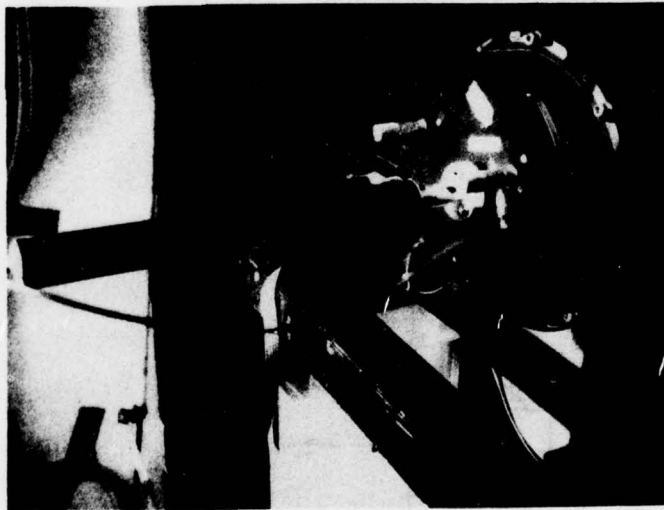
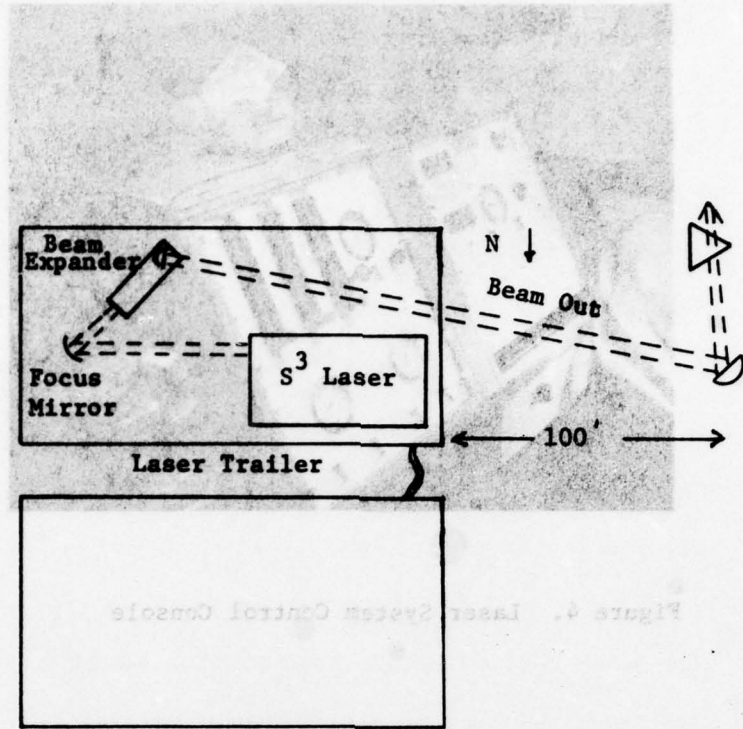
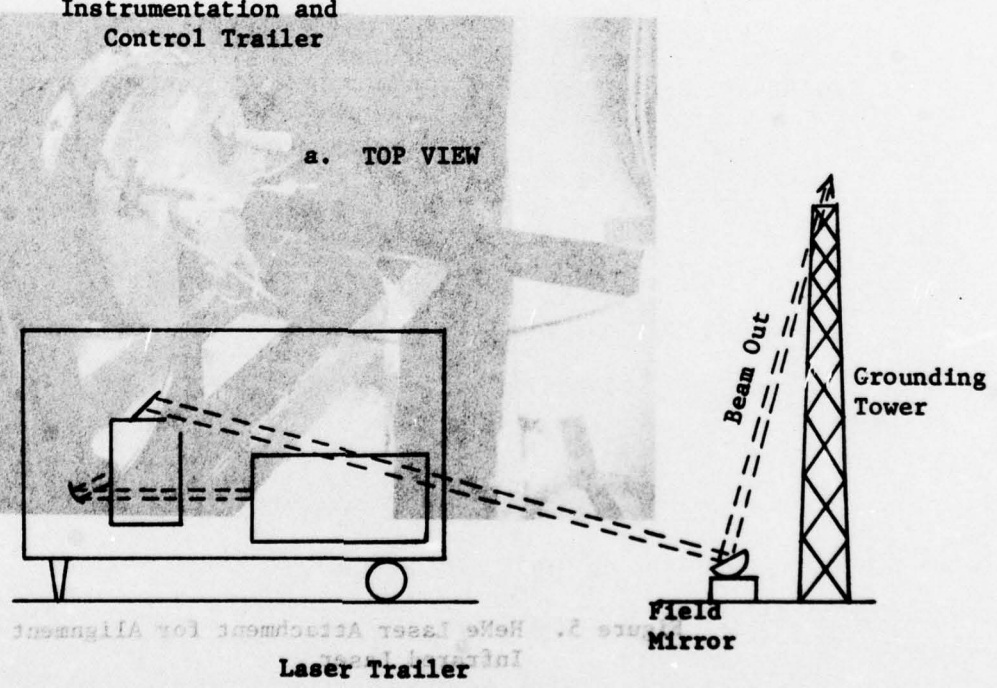


Figure 5. HeNe Laser Attachment for Alignment of Infrared Laser



a. TOP VIEW



b. SIDE VIEW

Figure 6. Facility Layout

**Figure 7. Beam Expanding Cassegrain Telescope and Pointing Mirror**

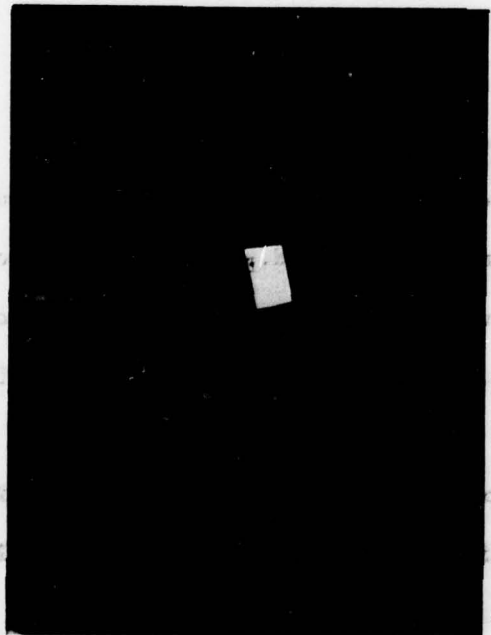
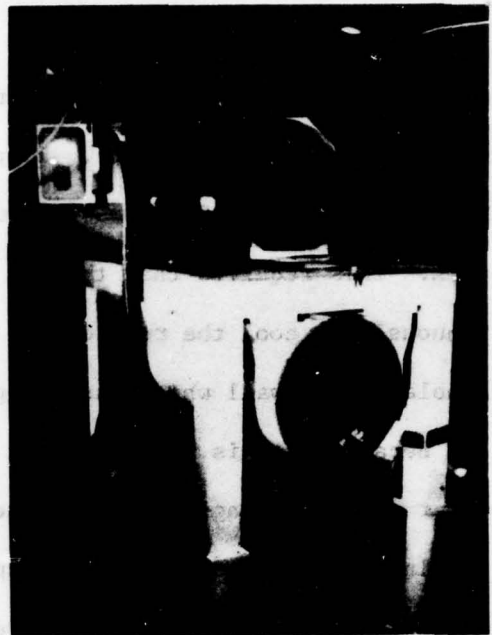


**Figure 8. Flat Field Mirror  
(Note Tower Electrodes  
in Rectangular Area of  
Reflection)**

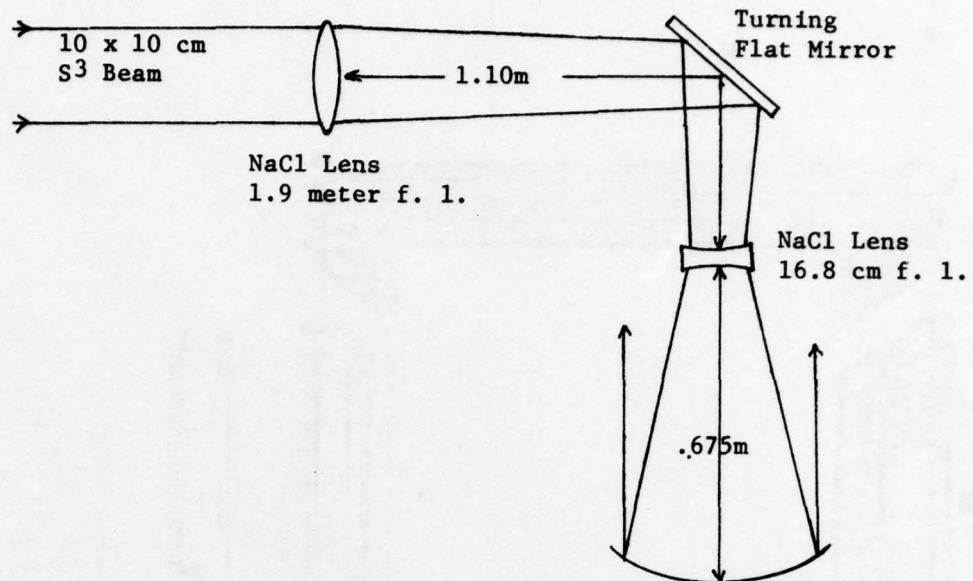
a 3 x 3 cm cross sectional area and then re-expand it to 25 x 25 cm at the field mirror (See Figure 8). To protect the salt lenses from the high ambient humidity, dry heated air was circulated continuously (24 hours a day) around them. This required that the air conditioning system be also operated continuously to cool the rest of the equipment. The laser was projected through a hole in the wall which was plugged when experiments were not in progress.

Because in this configuration the lenses could not withstand full laser power without damage, power was reduced and tests were conducted using only the laser generated gain switch spike output.

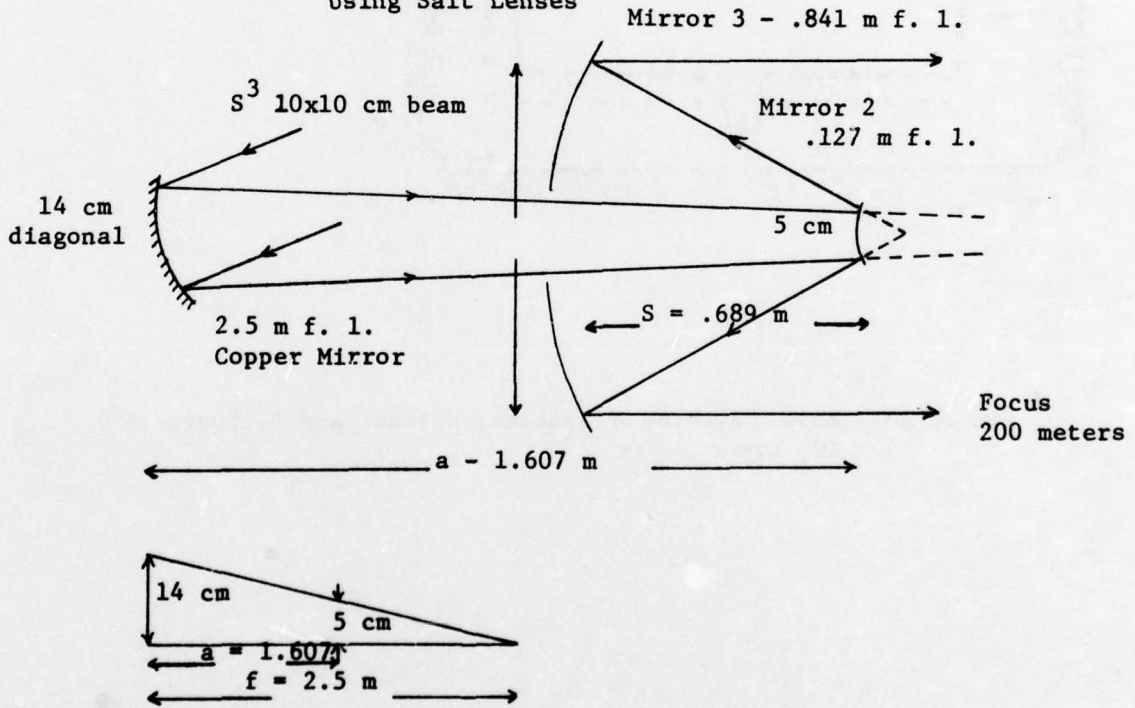
In an attempt to increase power at the focal point, the secondary mirror was reinstalled in place of the double convex salt lens and the expander was returned to its original position. The other salt lens was replaced by a 15 cm diameter concave copper mirror with a 5 meter radius of curvature. The dimensions and relative position of the optical elements along the calculation made to derive these dimensions are given in Figure 9.

The power of the laser was then increased to over 350 joules with a pulse duration of 1 microsecond and the experiments continued. The convex mirror finish was damaged by the beam and was twice rotated 120° in its holder to move the damaged surface out of the beam. The beam shape at the output of the laser and at the convex mirror are shown in Figure 10.

Figures 11 and 12 are a night time exposure of the laser beam path emitted from the semi-trailer and, after reflection off the field flat mirror, illuminating the tower electrodes and proceeding out into the night sky.



a. Optical Configuration of Expander System Using Salt Lenses



b. Optical Configuration of Expander System Using All Mirrors

Figure 9. Dimensions and Relative Positions of Optical Elements

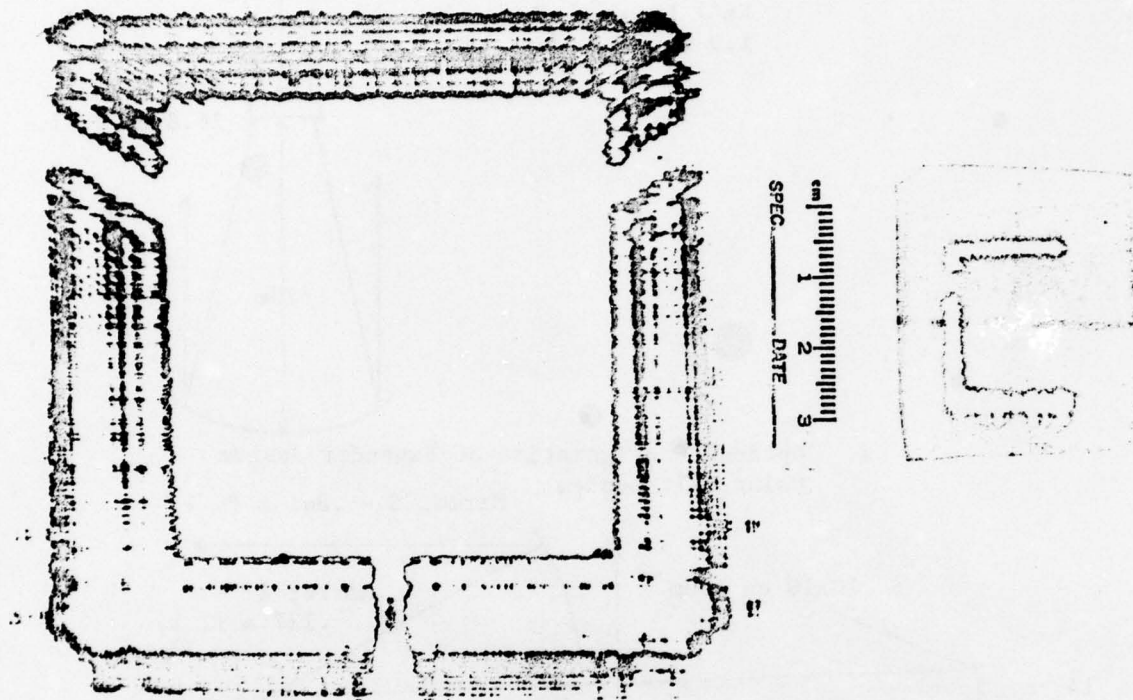


Figure 10. Beam Patterns of Systems, Science and Software (S<sup>3</sup>)  
CO<sub>2</sub> Laser.

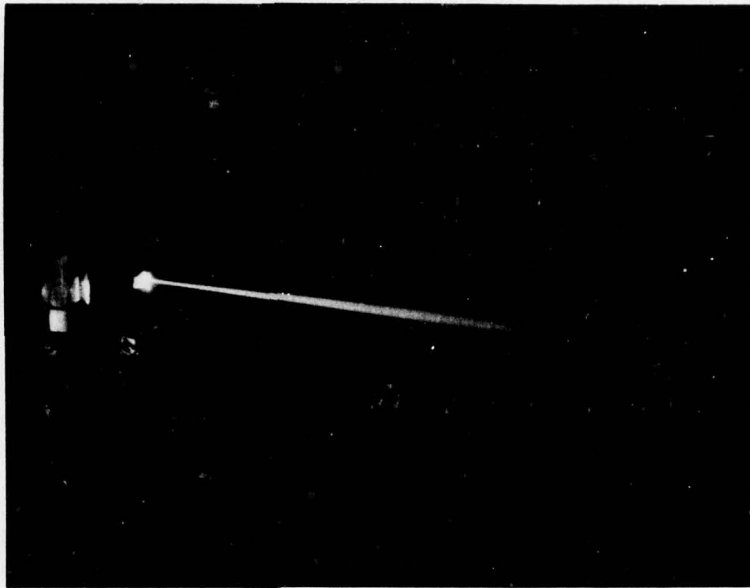


Figure 11. Beam Path from the Semi-Trailer Arrangement



Figure 12. Beam Path Illuminating Tower Electrodes and Propagating Outwards

#### 4. TEST INSTRUMENTATION

Detecting and analyzing equipment included: (1) a current transformer (CT) capable of 100,000 amp with a reduction factor of 6,800 to 1 (the CT was installed around one of the tower's uprights as shown in Figure 13), (2) a magnetic field detector (Fig. 14) aligned for maximum sensitivity along the laser beam path, (3) an electric field dipole antenna (Fig. 15) placed atop the control van, (4) a potential gradient field mill (Fig. 16) calibrated by the Air Force Geophysics Laboratory (AFGL) positioned directly under the beam path, (5) a prototype "Stormscope" (Fig. 17) that displays relative direction and approximate range of electrical activity from a combined E-field and ADF antenna system.

The detected signals were connected to BIOMATION Model 610B Transient Recorder for later playback and examination on a Tektronix 5000 series Oscilloscope. This setup displaying a typical signal response is shown in Fig. 18. To electrically isolate the instrumentation from the recording equipment, fiber optic coupling was used.

#### 5. TEST PROCEDURES

The LILE procedure was intended to optimize the chance of attaining a lightning discharge. Having all controls inside the van with the detectors and monitors allowed real time control over the equipment. The potential field gradient was monitored to detect charge accumulation overhead. As this value started increasing, both the laser and Marx generator were charged and readied for firing. At high field readings (favorable discharge conditions), the system would be fired. A thirty second waiting period for lightning discharge would be employed before repeating the procedure.

Procedures were developed for performing a number of small scale experiments while climatic conditions were not suitable for the formation of active

Figure 13. Current Transformer (CT)  
Installation

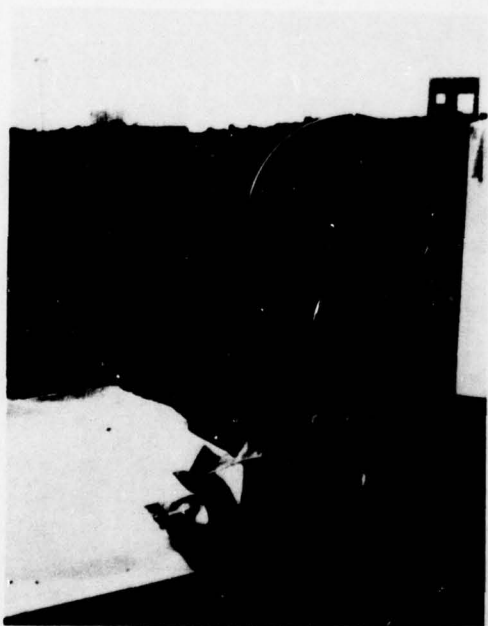
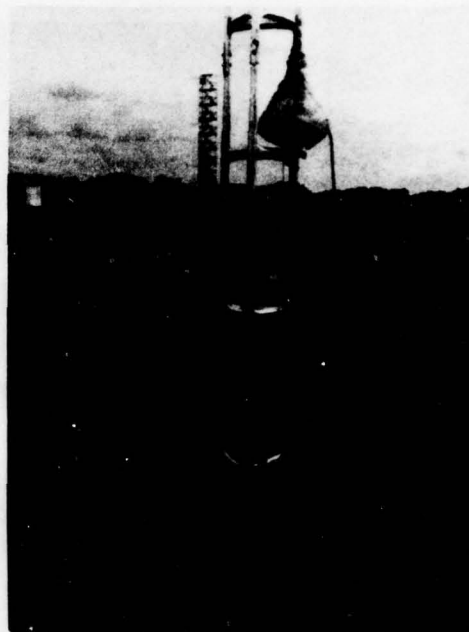


Figure 14. Magnetic Field  
Detector

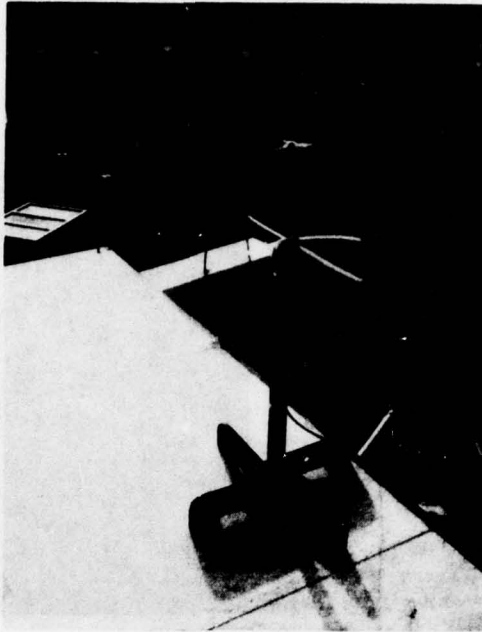


Figure 15. Electric Field Dipole



Figure 16. Potential Gradient Field Mill

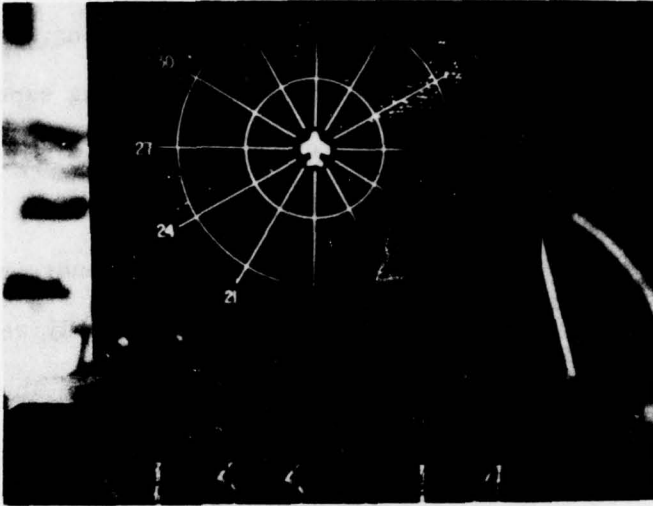


Figure 17. Stormscope Display

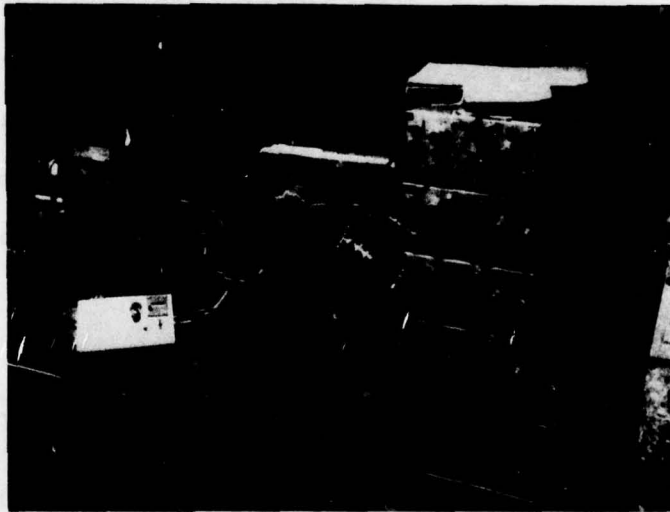


Figure 18. Transient Recorder and Oscilloscope Setup with a Typical Signal Display

thunderstorms. These included a spark-gap triggering, laser effects on electromagnetic fields and laser power/energy scaling experiments.

a. Spark-Gap Triggering Experiment Procedure

Two five inch diameter aluminum corona balls were attached to the positive and negative electrodes of a 100 KV Marx generator power supply and spaced to result in an air spark gap. The gap assembly was placed in the laser beam path and aligned using burn patterns on the Thermofax paper at the spark gap. The voltage required for arc discharge was determined and repeated to insure that the gap was stable and free from fluctuation. The gap was then charged to a slightly lower voltage and the laser beam pulsed between the corona balls. An arc discharge occurred. This process was repeated until no arc discharge occurred to determine the limit of the gap's breakdown voltage due to the laser energy. The laser's optical propagation system was then altered to move the beam's focal point and thereby change the energy density of the beam within the spark gap. The entire process of gap breakdown testing was repeated to investigate the energy/power dependency of the breakdown voltage reduction phenomena. A diagram of the spark gap arrangement is shown in Figure 19.

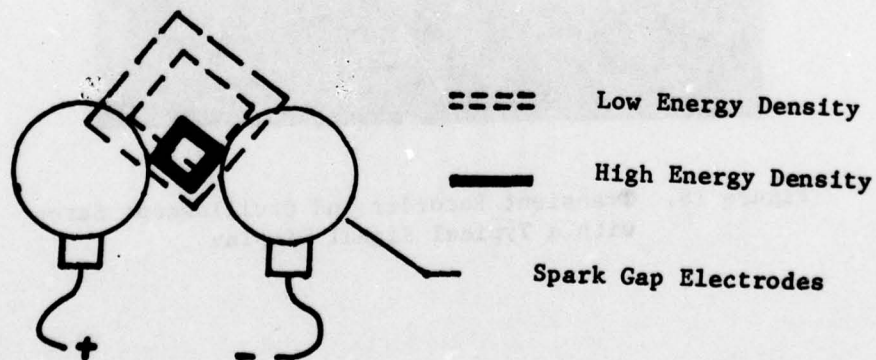


Figure 19. Laser Triggered Spark Gap Arrangement

b. Electromagnetic Field Effects Experiment

The laser beam was focused at different positions along the beam path and the resulting effects were compared on oscilloscope tracings. This isolated the effects due to the beam itself from those of the associated power supply equipment. In addition, a field-mill calibrated by the Air Force Geophysics Laboratory was located under the horizontal leg of the beam to measure any disturbance to the potential field gradient.

A megavolt Marx generator (Figure 20) was used to pulse the grounding tower in hopes of promoting streamering at the tower top electrodes. When discharged simultaneously with the laser, it was hoped the chances of inducing lightning would increase. The Marx generator was connected to the tower below the current transformer (closer to ground) so that any current detected would be moving towards the top, away from ground.

c. Laser Power/Scaling Experiment

Although the exact contributions from laser power versus laser energy on the pathway channeling effect are not certain, it appears that the more significant parameter for this experiment was the laser power. This is determined by the fact that present hardware can produce required laser powers at longer pulse lengths more readily than the high required laser energies at the shorter pulse lengths. These pulse lengths correspond to the power and energy dependent sides of the clean air breakdown curve in Figure 21 (taken from Reference 1). The CO<sub>2</sub> laser wavelength was chosen due to the combined high energies and powers available from present devices as well as the relatively low breakdown threshold of air due to cascade ionization at 10.6 microseconds. The comparative effectiveness in wavelength where multiphoton ionization predominates (as in UV lasers) were not addressed due to the nonavailability of high-power devices at those wavelengths.

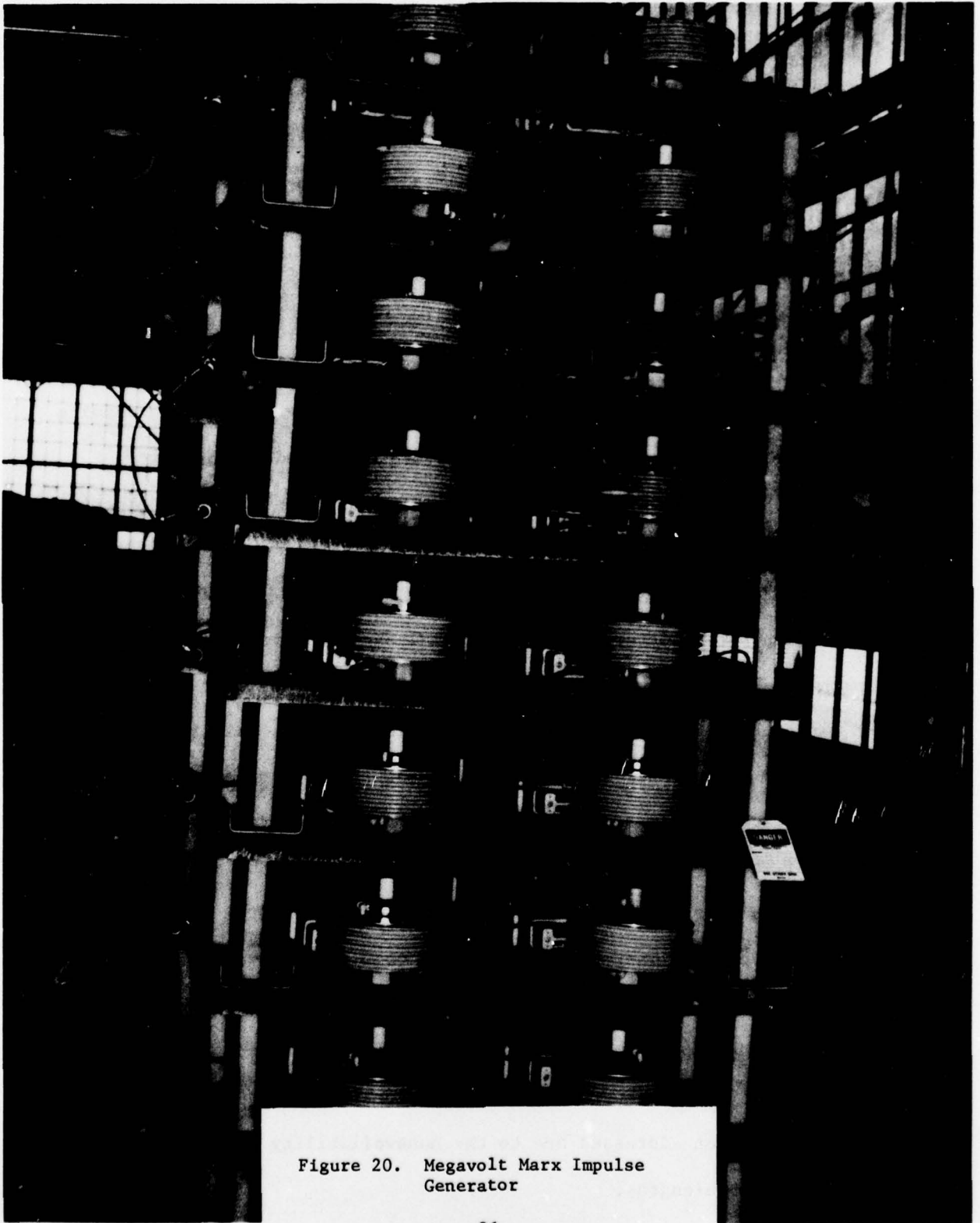


Figure 20. Megavolt Marx Impulse Generator

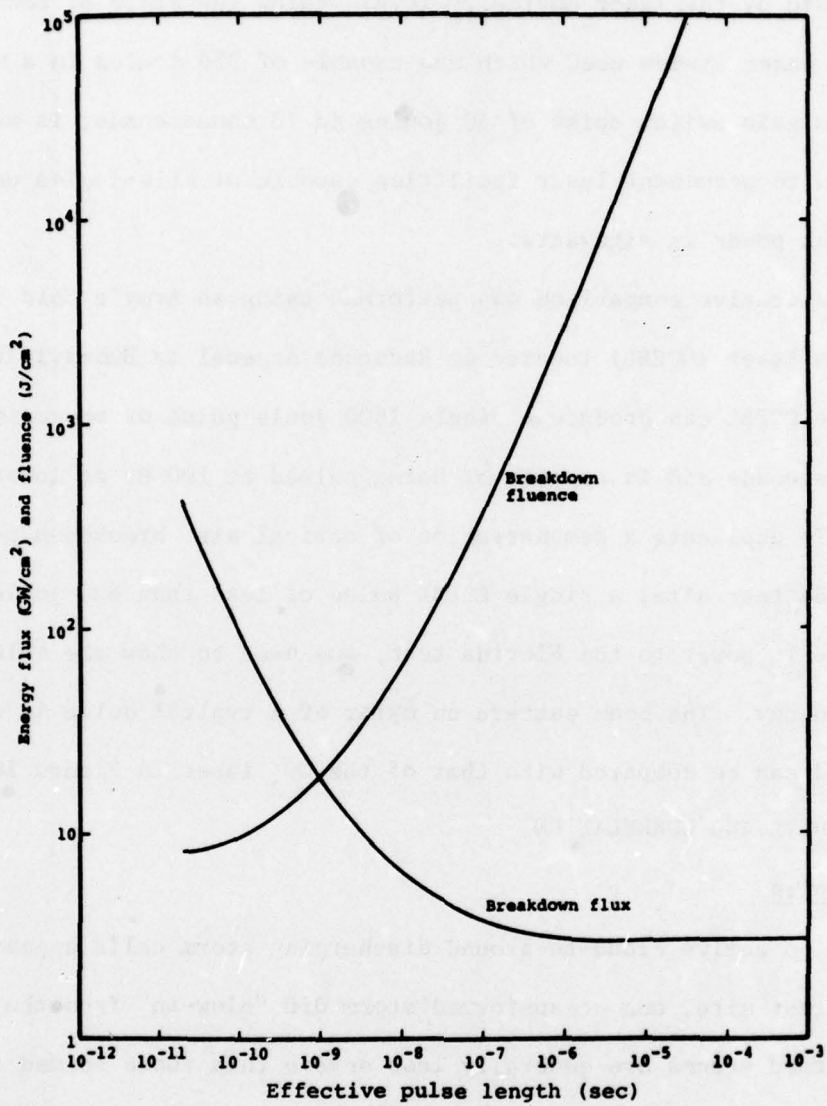


Figure 21. Breakdown Criteria, Clean Air at 10.6 $\mu$ m  
(Taken from Reference 1).

The requirements for a transportable laser system limited the size of the device and its power supply and restricted the power and energy provided by the laser device to levels below the state of technology. The laser system used which was capable of 350 joules in a microsecond with a gain switch spike of 40 joules in 70 nanoseconds, is weak when compared to permanent laser facilities capable of kilo-joules energy levels or peak power in gigawatts.

A qualitative comparison was performed using an Army's Cold Cathode Electron Beam Laser (CCEBL) located at Redstone Arsenal in Huntsville, Alabama. The CCEBL can produce a single 1600 joule pulse of approximately 2 to 3 microseconds and is capable of being pulsed at 100 Hz at lower energies per pulse. To duplicate a demonstration of optical air breakdown performed at the Florida test site, a single CCEBL pulse of less than 600 joules, which is comparable in power to the Florida test, was used to show the value of additional energy. The beam pattern on mylar of a typical pulse is shown in Figure 22 and can be compared with that of the CO<sub>2</sub> laser in Figure 10.

## 6. TEST RESULTS AND CORRELATION

### LILE Results

Although no active cloud-to-ground discharging storm cells appeared over the Florida test site, one ocean-formed storm did "blow-in" from the ocean. The ocean-formed storms are generally less severe than those formed from thermal heating over land during the same season. As this storm rolled in from the ocean, distant thunder and the glow of high altitude cloud-to-cloud strokes were observed. However, no cloud-to-ground discharges were noticed in the vicinity of the test site.

The storm clouds appeared to roll in as frontal waves, parallel to the coastline, with 5-10 minutes between the waves during the hour-long storm.

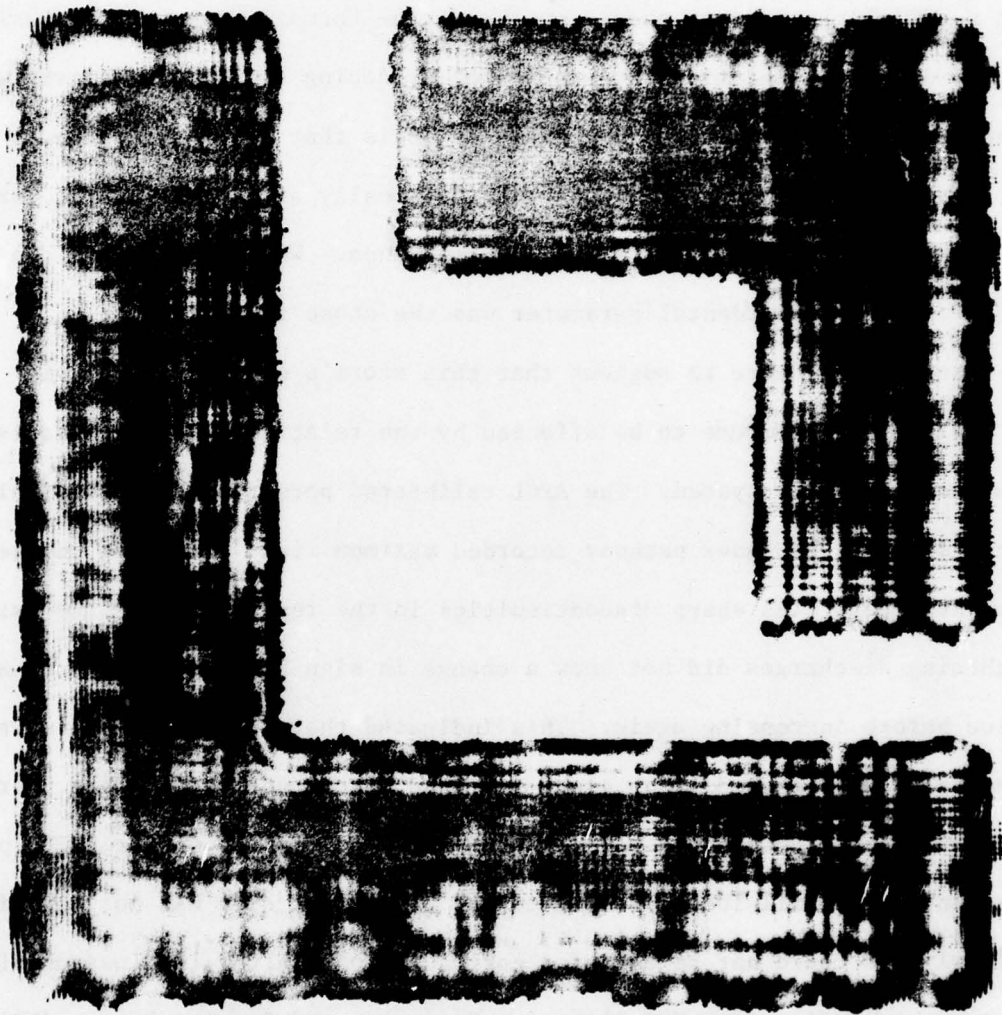


Figure 22. Beam Pattern of Army's Cold Cathode Electron Beam Laser (CCEBL).

Both the laser and the Marx generator were fired simultaneously as the clouds passed overhead. No cloud-to-ground discharges resulted; however, the random thunder of high altitude strokes continued. The laser and the Marx system were fired periodically after about 3-4 minutes charging time. As the parallel cloud waves passed overhead, the formations began to dissipate in the area over the middle of the site, producing two separate waves which proceeded inland. One possible explanation is that the laser and Marx generator were introducing enough ionization to locally affect the charge carriers in the vicinity and cause the cloud disturbance. Whether this was the case or some other coincidental parameter was the cause is not known.

There is evidence to suggest that this storm's electrical activity was at too high an altitude to be affected by the relatively short effective range of the laser system. The AFGL calibrated potential gradient field mill located below the laser pathway recorded maximum field gradients on the order of 2 KV/meter. The sharp discontinuities in the readings associated with lightning discharges did not show a change in sign but only a reduced absolute value before increasing again. This indicated that these readings were associated with more distant cloud-to-cloud discharges rather than nearby cloud-to-ground discharges. The Number 19 Kennedy Space Center (KSC) potential gradient field mill located close to the laser test site was not functioning properly and could not be used for corroboration. After termination of the storm, the reading from KSC Lightning Detection and Ranging System (LDAR) was examined to confirm the electrical activity present over the site. The lowest altitude of recorded electrical activity over the site was 20,000 feet, many times the effective range of the 500 meter or even a 1000 meter beam path. At this distance, a continuous conductor would have only a marginal effect and a preferential path an insignificant effect. The closest confirmed

cloud-to-ground discharge was approximately 5 miles west by northwest of the site.

a. Spark Gap Triggering Results

The data obtained in this experiment is presented in Table 1. The low energy values in the table were mathematically calculated using geometric optics since the 1 millisecond pulse energy density was too low to obtain burn patterns using the thermofax paper method.

TABLE I

SPARK GAP TRIGGERING EXPERIMENT RESULTS

<u>Laser Energy</u>	<u>Self-Breakdown</u>	<u>Gap Potential</u>	<u>Arc</u>	<u>Limit/% Reduction</u>
5 j/cm <sup>2</sup>	24.5 KV	22.5	yes	
		22.	yes	
		21.5	yes	
		21.	yes	
		20.5	no	20.75/15%
		20.	no	
		20.	no	
20 j/cm <sup>2</sup>	25 KV	21.	yes	
		20.5	yes	
		20	no	20.25/19%
		20.	no	
		20.5	yes	

The significance of these results is that the gap's breakdown voltage was positively reduced even though the concentration of laser energy was two orders of magnitude lower than that required for arc breakdown even under optimistic

conditions. This indicates that even a low level of laser irradiation in the presence of an electric field has the tendency to form a preferential pathway for electric flow (arc current). These results collaborate documented results by other experimenters with laser triggered switches and guiding long arc discharges (References 1, 7 and 8). The implication is that a continuous column of ionization from cloud-to-ground is not required to induce a lightning discharge and carry it to the desired ground point. It appears that lower intensity laser radiation over a long, gradual, focus would form an adequate preferential path for the intense field of a nearby pilot leader to seek and follow to discharge. These reduced power levels correspondingly reduce the beam handling and propagation problems and are within the state-of-the-art of present day laser technology.

There are several possible explanations for the above phenomena. For a laser pulse shorter than thermal or convective diffusion times but longer than acoustic expansion times, an isobaric heating model can be used following the equation:

$$\rho_1/\rho_0 = \frac{7}{2} P / (\frac{7}{2} P + (e/v)) \quad (1)$$

$\rho_1$  = final gas density

$\rho_0$  = initial gas density

p = pressure

e = laser energy absorbed

v = volume of gas

The effect of low level ionization is enhanced by the existence of an electric field. Propagating streamers have been measured approaching  $10^9$  cm/sec, compared to velocities of  $10^6 - 10^7$  cm/sec for electron avalanches without laser induced breakdowns. This is a strong parameter for

localized phenomena as spark gaps and should be adaptable to the realistic case of a natural pilot leader's intense field. The growth of charge carriers ( $n_x$ ) for this application is governed by the equation:

$$n_x = n_o e^{\alpha x} \quad (2)$$

$n_o$  = initial concentration

$\alpha$  = Townsend's first ionization coefficient

$x$  = distance of propagation

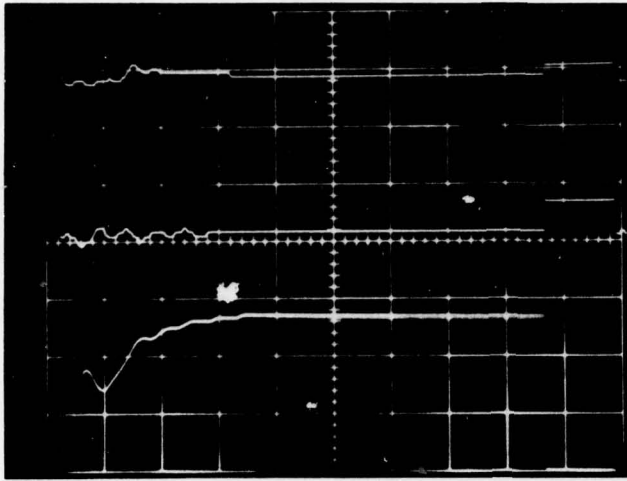
The initial concentration is determined by the laser power and the target that is absorbing that power. For the case involving electrodes with laser energy incident upon them, electrons and ions of thermionic origin are emitted. In the atmosphere, the laser energy first affects the particulate and aerosol "impurities" far below clean air breakdown power levels. The ionization extends radially and increases through the duration of the laser pulse. Gradual focusing compensates for the power loss due to propagation resulting in a long column of low level ionization. Admittedly, the initial concentration is less than that emitted from a laser irradiated electrode due primarily to the transmissivity of air. Further analyses may determine that it be more desirable to use a laser of a frequency that is more readily absorbed by the air. However, the trade-offs of power available vs. power required at those frequencies is another consideration. A possible benchmark for required charge carriers reported by Loeb<sup>9</sup> was that  $10^3$  ions/cm<sup>3</sup> are needed to modify normal streamer velocity. Also, in the realistic case, the electron/ion density appears not as important as the space gradient of that density. This further supports the premise that a preferential pathway can be generated below laser intensities needed to cause optical breakdown of the air.

b. Electromagnetic Fields Effects Results

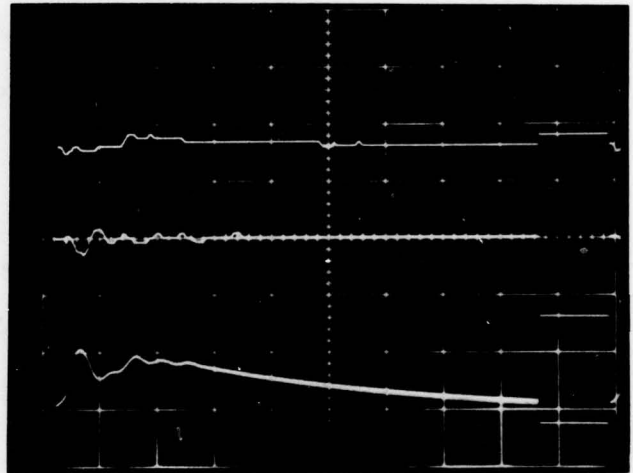
The laser effects on the nearby electric and magnetic fields and the potential field gradients were measured. Since these measurements were obtained in reasonably clear weather (field mill reading of 600 v/meter), the laser effects with regard to potential field strength could not be evaluated. Therefore, whether or not the effects would be increased due to the stronger fields prevalent in an active thunderstorm is not certain.

The oscillograms in Figure 23 are typical responses for a beam focused at 200 meters, the tower top (80 meters) and the horizontal leg (20 meters), respectively. The 20 meter focus resulted in a laser initiated air breakdown arc visible on television monitors and was recorded as a pulse on the Stormscope.

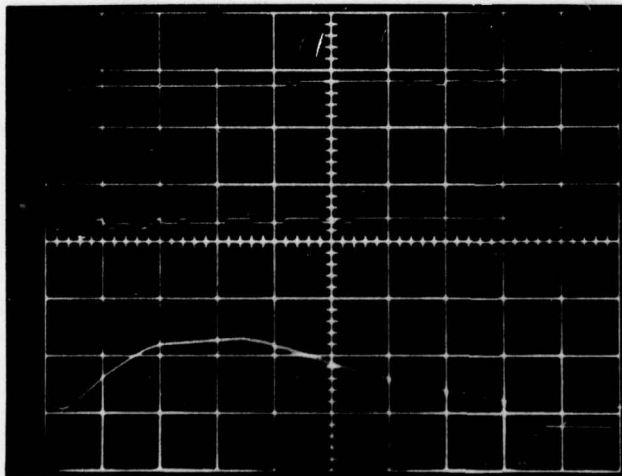
The top trace of the oscillograms is the response from the current transformer on the grounding tower set on 10 mv/cm sensitivity. The consistent low reading is attributed to noise pick-up on the signal transmission lines rather than a current flowing in the tower. The center trace is the response of the loop dipole E-field sensor antenna at 20 mc/vm sensitivity. Again the low value shows a negligible effect due to altering the laser focal point. The bottom trace is the response of the H loop sensor whose signal has been integrated to result in the H-field. Due to the equipment used for integration, only the first 50  $\mu$ sec of the trace should be considered. Time scales for all oscillograms are 25  $\mu$ /cm. The H-field sensor sensitivity was set at 10 mv/cm. The greater effect from the laser focus can be seen on the H-field tracings. Comparing the traces, the most distant focus condition resulted in the steepest risetime and the highest amplitude. The intermediate position did not have as steep a risetime and levels off earlier in an



a. Potential field gradient traces with beam focused at 200 meters.



b. Potential field gradient traces with beam focused at 80 meters (tower top)



c. Potential field gradient traces with beam focused at 20 meters (horizontal leg).

Figure 23. Typical Response at Three Beam Focus Distance

oscillatory fashion. The closest focus condition that terminated in an air breakdown arc, had a very gradual rise and did not appear to oscillate.

In addition, a potential field mill gradient calibrated by the Air Force Geophysics Laboratory was located under the horizontal leg of the beam to measure any disturbance to the potential field gradient. Each laser firing resulted in a pulsed increase of the field gradient of approximately 150 v/m. Since these readings could not be compared to a stormy (strong field gradient) day, it is not certain whether this is an explicit value or a percentage increase of the existing field strength. The conclusion is that the laser beam affected the surrounding fields but, at the powers and field strengths of the experiment, that effect was minor and could be obtained more readily by other means as described later.

Figure 24 is an oscillogram of the current transformer response to a Marx discharge of 20,000 amps. With a reducing factor of 6,800 to 1, the current transformer detected 1,900 amps. About 10% of the total current dumped into the tower was away from ground toward the tower top electrodes.

The effect that the Marx discharge had on the fields was also measured. An oscillogram of the electric and magnetic field response due to the Marx discharge is shown in Figure 25. With the sensitivity at 4 v/cm and 2 v/cm, respectively, the resulting effect to the surrounding fields is orders of magnitude greater than those caused solely by the laser, at least at the laser powers tested. However, by careful alignment of the Marx produced fields and simultaneous laser firing, a benefit to the lasers "channeling" effectiveness may be realized (Reference 10).

#### c. Power/Energy Scaling Results

The Florida demonstration involved using only the gain switch spike and focusing that output to cause optical breakdown as distant from the laser

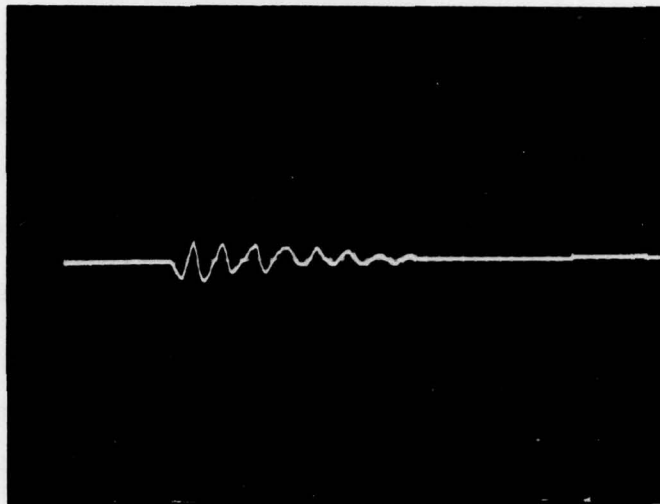


Figure 24. Current Transformer Response to a Marx Discharge of 20,00 Amps.

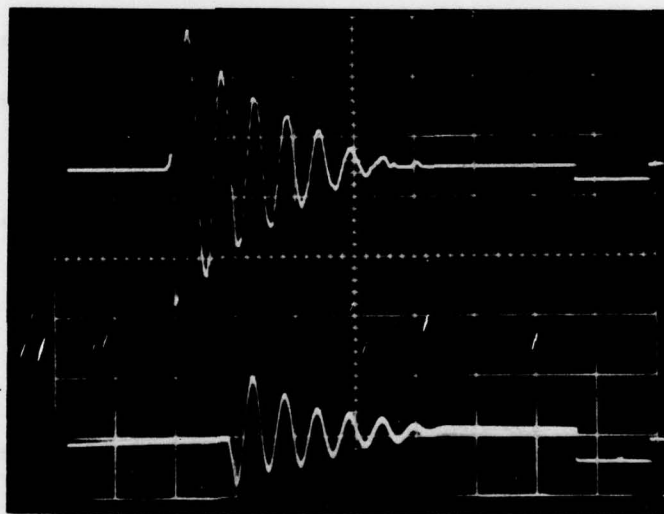


Figure 25. Electric (Top Trace) and Magnetic (Bottom Trace) Field Responses to Marx Discharge

as possible. A calculated value of 25 joules was transmitted through the optical system to initiate air breakdown. A single spot "arc" with a faintly audible "snap" resulted when the output beam was focused within 100 ft. of the laser. Beyond this distance, the attenuation and minimum spot size prevented the energy density to initiate a visible or audible spark unless it impinged on some material that would emit thermionic electrons or ions. However, this does not suggest that some level of ionization was not present.

When focused at about 500 ft., the CCEBL caused two separate spots of spark with one occurring at about 150 feet in front of the focus. Both spots were extremely bright and resulted in loud "cracks" clearly audible at 200 ft. distance. These spots' sizes were crudely estimated to be 2 - 5 inches in diameter, since there was no measurable reference. Figure 26 shows the Florida demonstration arc to the right of center photographed about 40 feet distant. Figure 27 offers a visual comparison of the CCEBL produced arcs. This figure is a downrange view superimposing the two spots. The distance from the camera to the first spot is about 300 ft.

Repetitive pulsing the CCEBL at 10 hertz produced a long series of "arc beads" as shown in Figure 28. The total length of the "beads" extended approximately 200 - 250 feet and is more representative of a uniform energy density throughout the region where the plasma beads form at some local inhomogeneity ("dirty air" particles). From these results, one can begin to estimate the effect if the CCEBL output were maximized for power and energy or if one of the still larger facilities were used for demonstration.

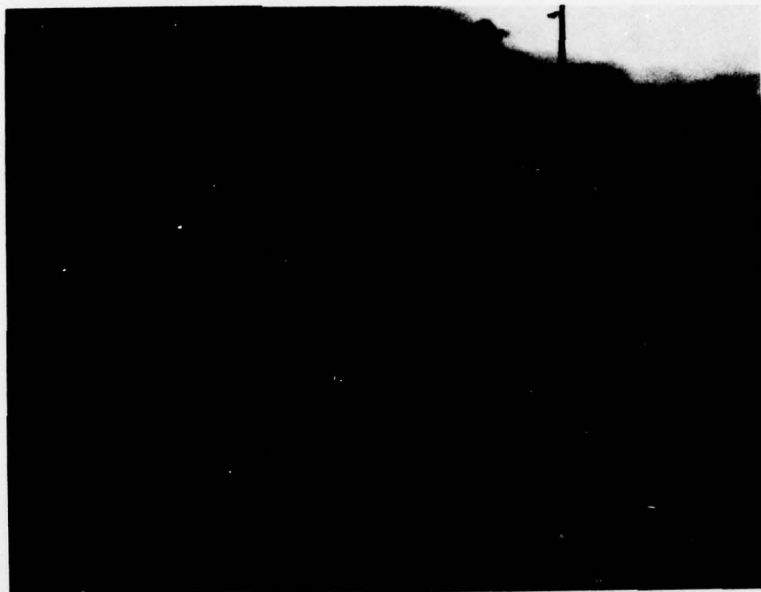


Figure 26. Florida Demonstration Arc



Figure 27. CCEBL Produced Arc

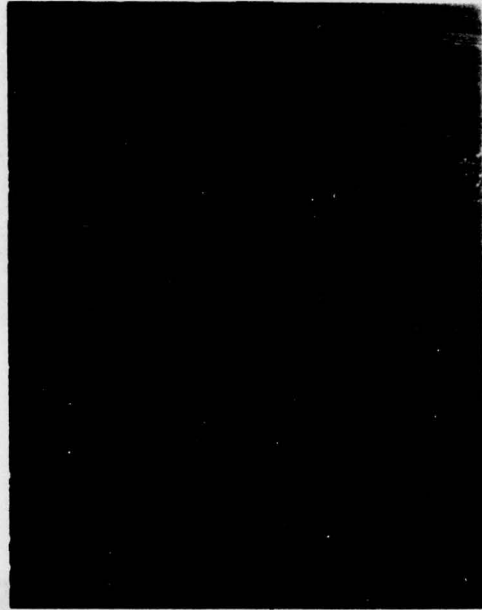


Figure 28. CCEBL "Arc Beads" Produced at 10 Hertz

### SECTION III

#### CONCLUSIONS AND DISCUSSIONS

Because conditions conducive to the formation of active cloud-to-ground discharging thunderstorms did not develop at the test site during the test period, the principal objective of the LILE program was not accomplished. Thus, the theoretical predictions remain undemonstrated. However, the other objectives of designing the experiment; selection of test locale, parameters and instrumentation; and development of test locale, parameters and instrumentation; and development of test procedures were all met and should significantly facilitate future experiments under favorable climatic conditions. In addition, secondary experiments involving spark gap triggering, electromagnetic field effects and power/energy scaling provided useful results which contribute to the understanding of the phenomena involved and also provide further insight in the technology. These contributions are summarized below:

1. Incident laser energy reduces the self-breakdown voltage in locally affected spark gaps. The triggering phenomenon was observed at a power density 1/100 of that required for optical breakdown of the air where no electrodes or electric fields were present.

2. Laser irradiation at the power and energies tested has only a marginal effect on the nearby electric field, magnetic field, and potential field gradient and thus is not expected to contribute significantly to triggering lightning by disturbing the prevalent field. Much greater field perturbations can be obtained by other means.

3. Evidence suggests that a continuous column of ionization may not be required to trigger a lightning discharge. Rarefaction of the air may provide a preferential pathway for a discharge to follow to ground.

Although the lack of appropriate thunderstorm activity prevented a conclusive demonstration of the Laser Induced Lightning Experiment, analysis of the phenomenon suggests that the concept should be feasible with suitable hardware. If such a system proves successful, possible applications besides environmental analysis could include local lightning protection for installations such as missile launch sites, weather modification, and possibly even control of tornados.

In recent years data has been collected suggesting that tornados are associated with extremely high levels of electrical activity. Two such data points were obtained with the LDAR on 28 January and 9 February 1973 (Reference 11). Figures 29 and 30 show the recorded LDAR signal strength (bottom trace) and number of pulses (top trace) versus time of day on days when tornados were sighted. These signals dramatically illustrate that electrical activity during a tornado is several orders of magnitude greater than the storm's average background count.

The effect of discharging this high level of activity on the behavior of the tornado is an interesting speculation. Possible applications such as these should justify further investigation towards the development of a laser-based lightning triggering system.

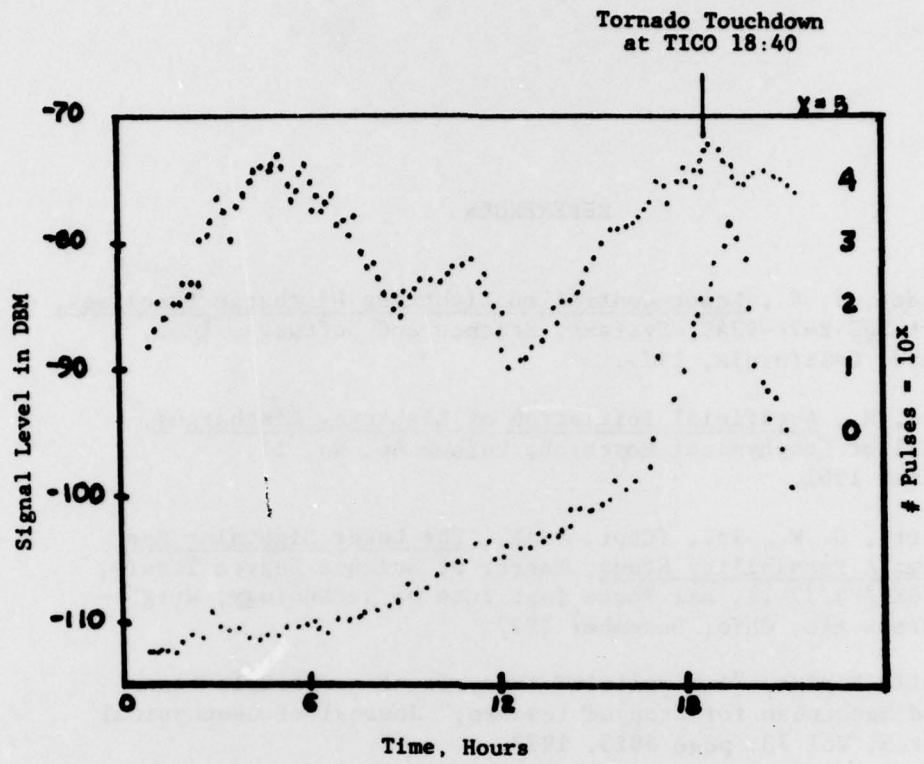


Figure 29. 24-Hour Signal Strength and Pulse Count Plot During a Tornado, January 28, 1973.

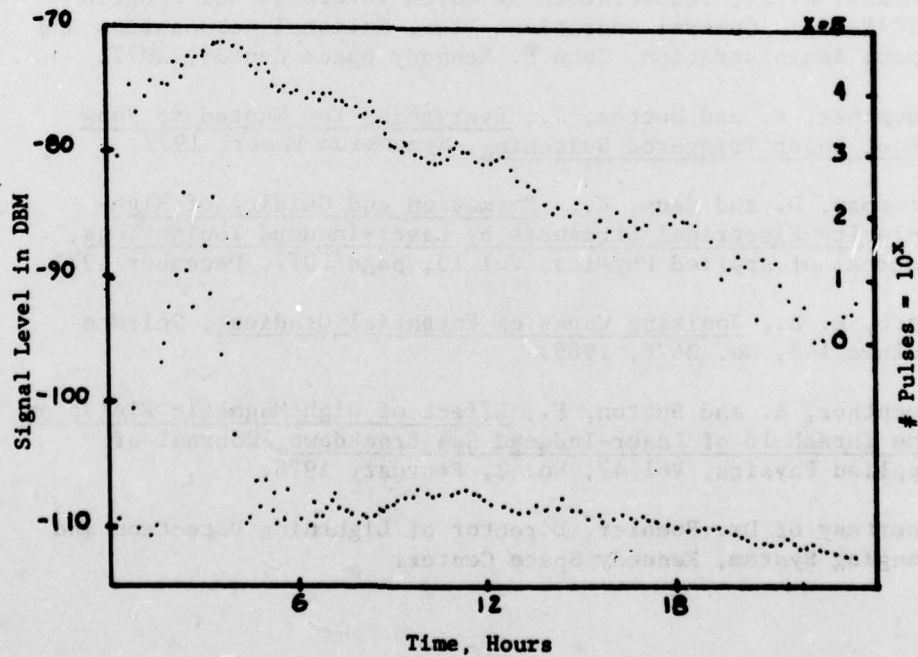


Figure 30. 24-Hour Signal Strength and Pulse Count Plot During a Tornado, February 9, 1973.

#### REFERENCES

1. Triplett, J. R., Laser-Controlled Lightning Discharge Processes, Report SSS-R-76-2749, Systems, Science and Software, Inc., Hayward, California, 1975.
2. Brooks, M., Artificial Initiation of Lightning Discharges, Journal of Geophysical Research, Volume 66, No. 11, November 1961.
3. Schubert, C. W., Jr., (Capt, USAF), The Laser Lightning Rod System: A Feasibility Study, Master of Science Degree Thesis, AFIT/GEP/PH/77-11, Air Force Institute of Technology, Wright-Patterson AFB, Ohio, December 1977.
4. Battelle Report, "A Simplified Analysis of a Possible Laser-Guided Mechanism for Stepped Leaders," Journal of Geophysical Research, Vol 73, page 5813, 1973.
5. Koopman, D. and Saum, K., Discharges Guided by Laser-Induced Rarefaction Channels, Physics of Fluids, November 1972.
6. Taiani, A. J., Thunderstorm Research International Program (TRIP-77): General Operations Plan, National Aeronautics and Space Administration, John F. Kennedy Space Center, 1977.
7. Guenther, A. and Bettles, J., Everything You Wanted to Know About Laser Triggered Switching, Symposium Paper, 1977.
8. Koopman, D. and Saum, K., Formation and Guiding of High-Velocity Electrical Streamers by Laser-Induced Ionizations, Journal of Applied Physics, Vol 15, page 2077, December 1973.
9. Loeb, L. B., Ionizing Waves of Potential Gradient, Science Volume 148, No. 3676, 1965.
10. Guenther, A. and Button, E., Effect of High Magnetic Fields on the Threshold of Laser-Induced Gas Breakdown, Journal of Applied Physics, Vol 47, No. 2, February 1976.
11. Courtesy of Dr. Poehler, Director of Lightning Detection and Ranging System, Kennedy Space Center.

APPENDIX

ANALYSIS OF SPECIFIC LASER-INDUCED IONIZED  
PATHWAYS AND TYPICAL DATA FOR  
ONE KILOMETER PATHWAY

The electron distribution produced by a laser lightning rod system is defined by the following equation (Ref 3):

$$w_F = \frac{1}{\sqrt{2}} \left[ w_L^2 - \sqrt{w_L^4 - 4 \left( \frac{\lambda z_F}{\pi} \right)^2} \right]^{1/2} \quad (A-1)$$

$$w_{L \text{ min}} = (2\lambda z_F / \pi)^{1/2} \quad (A-2)$$

$$w_B = \left[ R^2 w_L^2 + (1 - R^2) w_F^2 \right]^{1/2} \quad (A-3)$$

and

$$S(0,t)_{\text{max}} = S_T \frac{a^2 + (z_F - z_B)^2}{a^2 + z_F^2} \exp(A_T z_B) \quad (A-4)$$

where

$$R = (z_F - z_B) / z_F \quad (A-5)$$

and

$$a = \frac{\pi}{\lambda} w_F^2$$

The variables in the above equations are defined as follows:

$w_L$  - radius of final optical element for focusing the beam (cm)

$w_{L \text{ MIN}}$  - minimum radius of final element that will allow focusing at a given  $z_B$  (cm)

$w_B$  - beam radius at point where breakdown begins (cm)

$w_F$  - beam radius at beam waist (cm)

- $Z_F$  - distance of beam waist from final optical elements, focal lengths (m)  
 $Z_B$  - distance from final optical element to point where breakdown is initiated (m)  
 $S(o,t)_{max}$  - maximum flux intensity of laser pulse at final optical element (GW/cm<sup>2</sup>)  
 $\alpha, \beta$  - pulshape parameter  
 $\lambda$  - laser wavelength ( $\mu\text{m}$ )  
 $t_e$  - laser pulse length (sec)  
 $n_e$  - free electron density (electrons/cm<sup>3</sup>)  
 $Z_{max}$  - location of  $N_{e max}$  from final optical element (m)  
 $N_{e final}$  - electron density at end of computer calculation (electrons/cm<sup>3</sup>)  
 $Z_{end}$  - location of  $N_{e final}$  from final element (m)  
 $F$  - effect of focusing factor

These variables were used to reduce the electron distribution equation (Eq. 2) into a solvable form. To permit computer solution, values were specified for:

- $A_T$  - atmosphere attenuation coefficient (.41)  
 $S_T$  - breakdown threshold of air (3 GW)  
 $K$  - electron heating coefficient ( $2.35 \times 10^{-18} \text{ cm}^2$ )

These values were used in an iterative computer solution of the breakdown initiation and electron distribution equations (Eq. A-7 and A-8, respectively).

$$S_T = S_{max} \exp \int_0^{Z_B} [F(z) - A_T] dz \quad (\text{A-7})$$

and

$$\frac{1}{n(z)} \frac{dn(z)}{dz} = \frac{KS_T}{I} [Dt_z - Dt_1] + [F(z) - A_T] \ln \frac{n(z)}{n_{eo}} \quad (\text{A-8})$$

$$K [n(z) - n_{eo}]$$

where

$$Dt_1 = \frac{S(o, t_1) [A_T - F(z)]}{\partial S(o, t_1) / \partial t_1} \quad (A-9)$$

$$Dt_2 = \frac{S(o, t_2) A_T - F(z) + Kn(z)}{\partial S(o, t_2) / \partial t_2} \quad (A-10)$$

Tables A-1 and A-2 that follow are representative of the  
iterative solution by computer for two laser focal lengths ( $Z_F$ ) and  
common wavelength, pulse length, electron heating coefficient and  
atmospheric attenuation.

TABLE A-1

Typical Laser Rod Parameters for a 1-Kilometer  
Focal Length,  $Z_F$  (Taken from Reference 3).

$\lambda = 10.6$ $Z_F = 1000$		$t_P \approx 10^{-6}$ (II)		$K_A \approx 2.35 \times 10^{-18}$		$A_T = 0.41$	
$Z_B$	$W_L$	$n_e$ max	$n_e$ final	$Z_{max}$	$Z_{end}$	$S_{max}$	
125.0	8.21	3.81 E12	3.46 E12	162	240	2.79	
	10.21	1.05 E13	1.07 E13	140	168	2.50	
	12.21	1.20 E13	1.18 E13	140	164	2.46	
	14.21	1.25 E13	1.26 E13	140	162	2.44	
	16.21	1.27 E13	1.29 E13	140	161	2.43	
18.21	1.29 E13	1.26 E13	140	160	2.42		
250.0	8.21	3.45 E12	3.22 E12	288	377	2.60	
	10.21	1.21 E13	1.13 E13	264	289	2.04	
	12.21	1.41 E13	1.35 E13	279	283	1.95	
	14.21	1.38 E13	1.40 E13	260	281	1.91	
	16.21	1.40 E13	1.37 E13	260	280	1.89	
18.21	1.46 E13	1.46 E13	260	279	1.88		
375.0	8.21	3.10 E12	2.26 E12	429	528	2.43	
	10.21	1.37 E13	1.32 E13	392	408	1.62	
	12.21	1.56 E13	1.48 E13	384	403	1.48	
	14.21	1.76 E13	1.64 E13	384	401	1.43	
	16.21	1.81 E13	1.76 E13	384	400	1.40	
18.21	1.87 E13	1.85 E13	384	400	1.39		
500.0	8.21	2.18 E12	3.53 E11	558	765	2.30	
	10.21	1.40 E13	1.38 E13	510	531	1.25	
	12.21	1.95 E13	1.88 E13	508	524	1.07	
	14.21	2.17 E13	2.00 E13	508	521	1.00	
	16.21	2.31 E13	2.14 E13	508	521	0.97	
18.21	2.36 E13	2.40 E13	507	520	0.95		
625.0	8.21	6.06 E11	0	732	927	2.21	
	10.21	1.52 E13	1.46 E13	634	654	0.94	
	12.21	2.30 E13	2.19 E13	632	646	0.72	
	14.21	2.78 E13	2.65 E13	636	642	0.64	
	16.21	2.82 E13	2.91 E13	630	641	0.60	
18.21	3.04 E13	3.02 E13	630	640	0.58		
750.0	8.21	9.67	0	770	832	2.17	
	10.21	1.39 E13	1.17 E13	770	783	0.71	
	12.21	2.58 E13	2.38 E13	758	769	0.46	
	14.21	3.40 E13	3.31 E13	755	764	0.36	
	16.21	4.05 E13	4.02 E13	754	762	0.32	
18.21	4.45 E13	4.44 E13	754	761	0.30		
875.0	8.21	0	0	875	875	2.18	
	10.21	6.71 E12	8.24 E11	899	966	0.57	
	12.21	1.95 E13	1.68 E13	883	900	0.30	
	14.21	3.28 E13	3.13 E13	879	889	0.19	
	16.21	4.91 E13	4.66 E13	879	885	0.14	
18.21	5.73 E13	5.95 E13	877	883	0.11		

TABLE A-2

Typical Laser Rod Parameters for a 0.5 Kilometer Focal Length,  $Z_F$  (Taken from Reference 3).

$\lambda = 10.6$   
 $z_F = 500$      $t_E \approx 10^{-6}$  (II)     $K_A \approx 2.35 \times 10^{-18}$      $A_T = 0.41$

$Z_B$	W L	$n_e$ max	$n_e$ final	$z_{max}$	$z_{end}$	S max
62.5	5.81	1.07 E13	9.43 E12	78	106	2.72
	7.81	2.55 E13	2.42 E13	70	81	2.42
	9.81	2.78 E13	2.64 E13	74	79	2.38
	11.81	2.84 E13	2.84 E13	79	79	2.37
	13.81	2.68 E13	2.68 E13	78	79	2.36
	15.81	2.64 E13	2.62 E13	75	79	2.36
125.0	5.81	1.00 E13	9.51 E12	140	171	2.47
	7.81	2.67 E13	2.77 E13	130	142	1.89
	9.81	2.98 E13	3.11 E13	130	140	1.82
	11.81	3.24 E13	3.01 E13	130	139	1.80
	13.81	3.14 E13	3.20 E13	130	139	1.79
	15.81	3.19 E13	3.09 E13	130	139	1.78
187.5	5.81	9.10 E12	8.11 E12	204	239	2.25
	7.81	3.22 E13	3.15 E13	192	202	1.43
	9.81	3.70 E13	3.66 E13	192	200	1.33
	11.81	3.85 E13	3.82 E13	192	200	1.29
	13.81	4.03 E13	3.93 E13	192	199	1.28
	15.81	3.99 E13	3.85 E13	192	199	1.27
250.0	5.81	7.18 E12	5.80 E12	269	318	2.08
	7.81	3.62 E13	3.42 E13	254	263	1.04
	9.81	4.61 E13	4.46 E13	254	261	0.91
	11.81	4.93 E13	4.92 E13	254	260	0.87
	13.81	5.09 E13	4.92 E13	254	260	0.85
	15.81	5.15 E13	5.15 E13	254	260	0.84
312.5	5.81	5.12 E12	1.27 E12	339	429	1.94
	7.81	4.16 E13	3.73 E13	317	324	0.72
	9.81	5.55 E13	5.55 E13	321	321	0.57
	11.81	5.98 E13	5.65 E13	315	320	0.52
	13.81	6.43 E13	6.60 E13	315	320	0.50
	15.81	6.39 E13	6.73 E13	315	320	0.49
375.0	5.81	1.05 E12	0	426	516	1.86
	7.81	4.02 E13	3.61 E13	379	387	0.49
	9.81	6.63 E13	6.44 E13	377	382	0.32
	11.81	8.57 E13	8.46 E13	377	381	0.27
	13.81	9.52 E13	9.09 E13	377	380	0.24
	15.81	9.97 E13	9.08 E13	377	380	0.23
437.5	5.81	2.46	0	448	458	1.82
	7.81	2.65 E13	1.85 E13	444	457	0.35
	9.81	6.53 E13	5.65 E13	440	445	0.17
	11.81	1.06 E14	9.94 E13	440	442	0.11
	13.81	1.37 E14	1.29 E14	439	441	0.08
	15.81	1.65 E14	1.48 E14	438	440	0.07